WERNER DECONVOLUTION AND INTERPRETATION OF AEROMAGNETIC DATA OVER PARTS OF THE UPPER BENUE TROUGH, NIGERIA.

BY

Yusuf LECKY B.Sc.(Hons).

A thesis submitted to the Postgraduate School, Ahmadu Bello University, Zaria in partial fulfilment of the requirement for the award of the degree of Master of Science in Applied Geophysics.

Department of Physics
Faculty of Science
Ahmadu Bello University
Zaria

MAY, 1990

DEDICATION

This work is dedicated to my wife,

children and my senior brother,

Mr Christopher Z.A. Lecky.

DECLARATION

The report presented in this thesis is not a published, or an unpublished work of another author. It is the result of an original study carried out by this author. To the best of my knowledge, it has not been submitted in whatever form to any other institution, organisation or body other than the Ahmadu Bello University for the award of a degree. Where the work of others are made use of, such sources are appropriately acknowledged and referenced.

Yusuf LECKY

CERTIFICATION

This thesis entitled 'Werner Deconvolution and Interpretation of Aeromagnetic Data over parts of the Upper Benue Trough, Nigeria' by Yusuf LECKY meets the regulations governing the award of the degree of Master of Science of Ahmadu Bello University, and is approved for its contribution to knowledge and literary presentation.

---------- Date 6/8/90

(Name and Signature)
Dr. S.B. Ojo
Chairman, Supervisory Committee

---------- Date 10/8/90

(Name and Signature)
Dr. I.B. Osazuwa
Member, Supervisory Committee

---------- Date 15/8/90

(Name and Signature)
Prof. J. Adetunji
Head of Department

---------- Date 8-11-90

(Name and Signature)
Prof. D.I. Saror
Dean, Postgraduate School.

ACKNOWLEDGEMENT

I wish to express my gratitude and heartfelt indeptedness to Dr. S.B. Ojo for his unflagging supervision. I am particularly impressed by his penetrating judgement, intellectual and personal influence. Dr. I.B. Osazuwa, equally made invaluable contributions. I greatly appreciate his useful advice, support and encouragement at various stages. I am also appreciative of the encouragement and assistance offered by Professor J. Adetunji, Dr. C.O. Ajayi and Dr. M. Umego of Physics Department, A.B.U., Zaria.

I also wish to make special mention of Mary Momoh, Basil Nwosu and Abayomi Fagbemi for their assistance at various stages of this work.

Finally I must express my appreciation to my wife and children for their support, encouragement and patience throughout my study period.

ABSTRACT

The Werner deconvolution method of interpretation using aeromagnetic data along profiles has been used to carry out a basement study of parts of the Upper Benue Trough within latitudes 10°30'N to 11°30'N and longitudes 11°00'E to 12°00'E. Deconvolution was applied to profiles Spaced about 2 Km apart which made correlation of calculated depths from adjacent profiles possible. Depths which were consistent for adjacent profiles through the same anomalies were used in fitting magnetic basement surfaces to magnetic profiles and in preparing a magnetic basement contour map for the area.

The results show that the maximum thickness of the sediments lies between 1.4 Km and 2.0 Km with the deepest portion located between Wawa and Dukul, Some magnetic lineaments were delineated in the qualitative interpretation which match some of the lineaments interpreted by Ajakaiye et al (1986). These have been related to structural changes in the magnetic composition of the basement rocks. It was also observed that the basement topography cannot totally account for all the magnetic intensity variation which is attributed to the poor resolution of the produced basement map as well as the heterogeneous magnetic character of the basement rocks.

TABLE OF CONTENT

		Page
Title page		i
Dedication		ii
Declaration		iii
Certification		iv
Acknowledgment		v
Abstract		vi
Table of Contents		vii
List of Tables		ix
List of Figures		x
CHAPTER 1:	INTRODUCTION	1
1.1	General Background	1
1.2	Previous Geophysical Work in the Benue Trough.	2
1.3	Objective and Scope of study	5
CHAPTER 2:	GEOLOGY OF THE SURVEY AREA	7
2.1	Introduction	7
2.2	Palaeozoic and Precambrian Rocks	7
2.3	Cretaceous	10
2.4	Tertiary and Quaternary	11
2.5	Volcanic Activities	13
2.6	Structures	14
CHAPTER 3:	METHOD OF INTERPRETATION	16
3.1	Introduction to Aeromagnetic Method	16
3.2	The Werner Deconvolution Technique	19
3.2.1	Mathematical Derivations	20

3.3	Method of Application of Werner Deconvolution.	29
3.3.1	Results from Theoretical Model Studies	31
CHAPTER 4:	RESULTS AND INTERPRETATION	35
4.1	Introduction	35
4.2	Qualitative Interpretation	35
4.2.1	Correlation of Aeromagnetic Anomalies with the known Geology.	37
4.3	Werner Deconvolution of field Data	41
4.3.1	Profile Interpretation	43
4.4	Magnetic Basement Map	53
CHAPTER 5:	DISCUSSION AND CONCLUSION	57
5.1	Summary and Discussion of Results	57
5.2	Conclusion	59
	References	60
	Appendix	64.

LIST OF TABLES

TABLE 2.1:	Stratigraphy of Upper Benue	12
TABLE 4.1:	Flight Parameters	36
TABLE 4.2:	Input data for Werner deconvolution	42

LIST OF FIGURES

FIGURE	1.1	Geological map of Nigeria showing the area of study	2
	2.1	Geological map of Upper Benue	8
	2.2	Geological map of the study area, (after Carter et al., 1963)	9
	3.1	Geometry and spatial relation of the infinite dyke (after Gay, 1963)	21
	3.2	Geometry of thin dyke: (A) top view and (B) Cross section view	22
	3.3	Relationship between the total magnetic field and its components in y - z plare	25
	3.4	Interpretation of a theoretical basin model using Werner deconovolution method.	33
	4.1	Total magnetic field intensity of the study area.	38
	4.2	Combined geological and total magnetic field anomaly map.	40
	4.3	Correlation of field profiles	45
	4.4	Geological map showing position of field profiles.	46
	4.5	Interpretation of Profile L141	47
	4.6	Interpretation of Profile L142	48
	4.7	Interpretation of Profile L143	49
	4.8	Interpretation of Profile L144	50
	4.9	Interpretation of Profile L129 and L130. A case of uncorrelated depths for similar magnetic anomalies.	52

FIGURE 4.10 Geological map of study area showing the positions of depths used in preparing the magnetic basement map of the area. 54

4.11 Combined magnetic basement map and surface geology. 55

CHAPTER ONE

INTRODUCTION

1.1 General Background

The Benue Trough is a linear sedimentary basin 80 Km-150 Km wide and bounded on either sides by crystalline basement rocks (granites and gneisses) of Palaeozoic age. The trough is filled with strongly folded Cretaceous rocks whose ages range from Middle Albian to Maestrichtian (Carter et al., 1963). The north-eastern section of the trough is referred to as the Upper Benue Trough (figure 1.1).

Due to its economic potentials and structural significance in the context of plate tectonics and the world rift system, much attention has been focused on geological and geophysical investigations within the trough to study its origin, evolution, structural stratigraphy and its economic potentials (Cratchley and Jones, 1965; Ajakaiye and Burke, 1973; Offodile, 1976, 1977; Osazuwa, 1978, 1981; Adigbhje, 1979, 1981a,b; 1984a,b, 1985).

In the present survey the area of the trough under consideration lies within latitudes 10° 30'N to 11° 30'N and from longitudes $11^{\circ}00$ 'E to $12^{\circ}00$'E, covering parts of the Upper Benue Trough and a small portion of Chad Basin (figure 1.1.) The area is underlain by Precambrian rocks with a series of basic, intermediate and plutonic intrusives. Tertiary and recent basalts overlie the eastern part

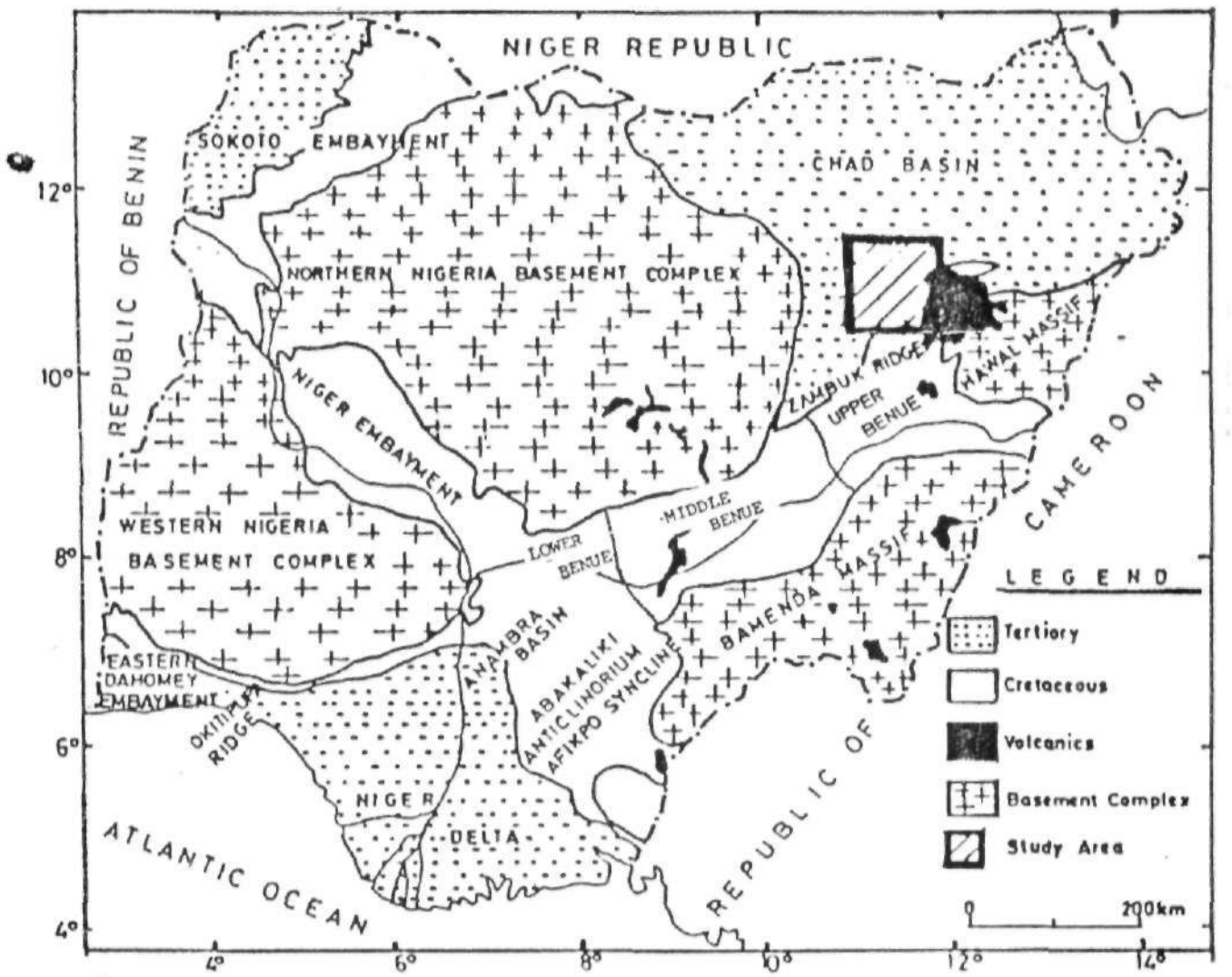


Fig. 1.1. Geological map of Nigeria showing the area of study.

and the rest of the area is overlain by Cretaceous sediments, Tertiary sandstones (the Kerri - Kerri formation) and Quaternary sandstones (the Chad formation) (Cater et al. 1963). A detailed geological description of the study area is given in Chapter 2.

1.2 Previous Geophsical Work in the Benue Trough

Previous geophysical studies of the Benue Trough have been mainly gravity method (Cratchley and Jones,1965; Artsybashev and Kogbe, 1975; Adighije, 1979; Adighije, 1981, b; Ajayi and Ajakaiye, 1981; and Osazuwa et al., 1981). From these studies it has been shown that the most prominent feature in the gravity field within the trough is a central positive anomaly with negative anomlies on either flanks. The axial gravity high extends along the entire length of Upper and Middle Benue. Considering available geological information and the gravity data, most of the earlier results have associated the central positive anomalies with intermediate and basic intrusion within the basement or sedimentary basin coupled with shallow basement. The negative anomalies were interpreted as being caused by Cretaceous sediments of various thicknesses (1.5 Km - 6.0 Km) and width (19 Km - 40Km) within the basement. There are also other interpretations which suggest the presence of faults in certain sections of the trough (Osazuwa, 1978; Ajayi, 1981; Okafo, 1982).

Not as much attention has been given to the interpretation of magnetic anomalies over the Upper Benue Trough as with gravity interpretation. Nevertheless, the results of the few magnetic investigations in the Benue Trough are comparable to those in gravity. Osazuwa et al., (1981) carried out a magnetic survey simultaneously with gravity survey along a NW-SE profile from Kaltungo to about 70 kilometers south of Numan, and along a N-S profile from Little Gombi to Yadim. They interpreted the magnetic lows as being caused by thick sedimentary deposits and magnetic highs as due to near-surface magnetic materials of abnormally high magnetic content. The sedimentary thickness range from 0.9 Km to 4.9 Km, with the greatest thickness of 5.9 Km recorded for sediments near Numan. Ofoegbu (1982, 1984a, 1984b) carried out a detailed aeromagnetic study of several isolated anomalies in the Benue Trough. In these studies he showed that although the anomalies over the Upper Benue can be independently accounted for in terms of either a basement of varied topography or instrusive bodies, they are best interpreted in terms of the combined effects of intrusive bodies and a crystalline basement topography at varied depths. He interpreted the intrusive bodies to have magnetization between 1.0 A/m and 2.8 A/m with a few cases below 1.0 A/m. These intrusives of widths varying between 2 Km and 30 Km were

interpreted to exist at depths up to 10 Km. On the other hand, the basement was interpreted to have depths ranging from 0.5 Km to 4.6 Km and magnetization between 0.24 A/m to 2.3 A/m or an average of 0.39 A/m. Other aeromagnetic studies include the aeromagnetic data analysis of the Benue Trough and the neighbouring Younger Granite Complexes, and some portions of the Chad Basin by Ajakaiye et al., (1986). These studies show the existence of narrow magnetic lineaments parallel to the margins of the Benue Trough.

More recently Nwogbo (1987) carried out a detailed depth interpretation of the Upper Benue using spectral methods. The results of the work show the presence of structures between depths of 9.4 Km and 31.5 Km, 4.4 km and 5.1 km, and from 2.0 km to 2.8 Km.

1.3 Objective and Scope of Study.

Previous studies by various workers in the Benue Trough show that there is need for a detailed investigation of the area using various geophysical methods with a view to throwing more light on these results. The area of the present investigation covers the intersection of four major sedimentary formations. These are Chad formation, Kerri-Kerri formation, Pindiga formation and Gombe sandstone. The area also covers a region which previous workers (Ajakaiye et al., 1986) have identified as being structurally significant because of the presence of a series of

parallel lineaments. The primary aim of this present investigation was therefore to carry out a detailed basement mapping of this region to determine the sedimentary thickness, and to investigate whether the structures suggested by other workers are reflected in the basement topography.

CHAPTER 2

GEOLOGY OF THE SURVEY AREA

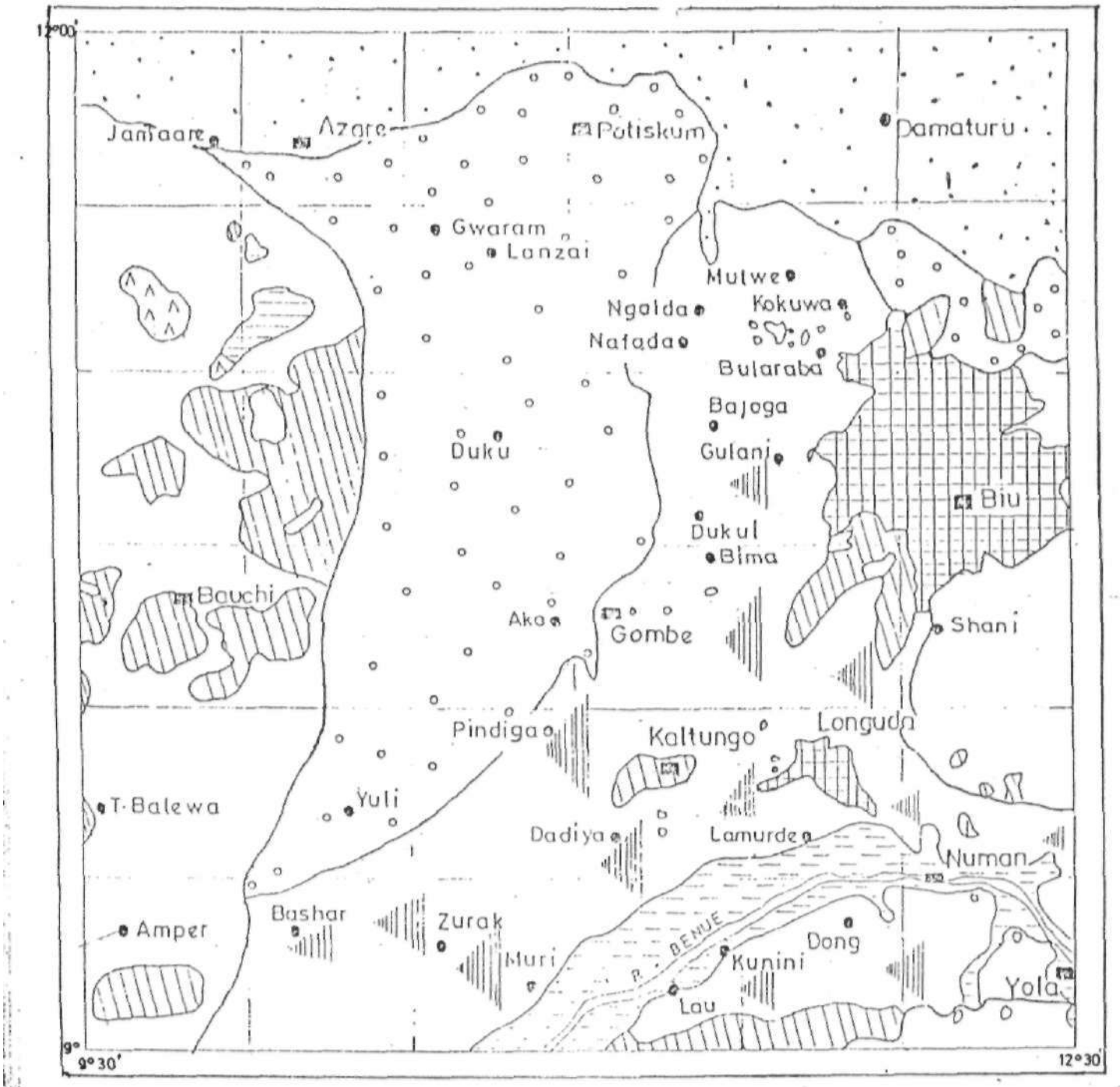
2.1 Introduction.

The geology described in this section covers an area of approximately 12,000 Km^2 lying between latitudes $10^{o}30'N$ and $11^{o}30'N$ and longitutute $11^{o}E$ and $12^{o}E$. The area includes parts of the Upper Benue Trough and the Chad Basin. The essential geological features of this region are shown in Fig. 2.1 and Fig. 2.2 and comprise sedimentary and volcanic rocks ranging in age from upper Cretaceous to Quaternary. It is underlain by gneisses, migmatites and metasediments of Precambrain age which have been intruded by a series of granitic rocks of late Precambrian to Lower Palaeozoic age. The geology of this area is well documented by Carter et al., (1963) and most of the information in this section have been derived from his work.

2.2 Palaeozoic and Precambrian Rocks.

The Palaeozoic and Precambrian rocks in this region include the Basement complex, Younger metaseidments and Older Granite series.

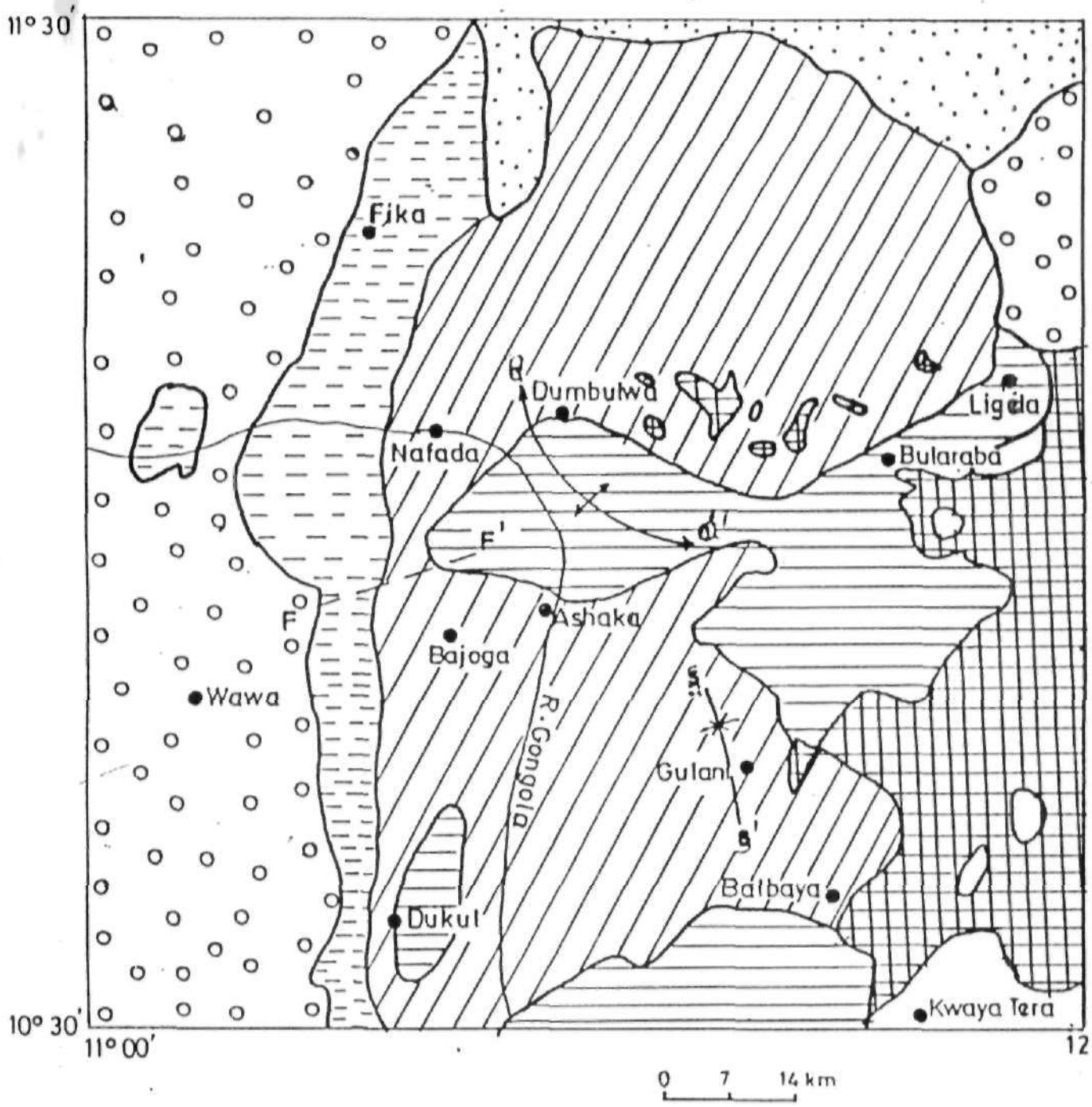
The Basement Complex comprises all rocks older than the Proterozoic metasediments. In this group are quartzites, schists, marble, basic calcareous



LEGEND

QUATERNARY	CHAD FORMATION	ALLUVIUM SANDS AND CLAYS
TERTIARY	TERTIARY TO RECENT VOLCANICS KERRI-KERRI FORMATION	BASALTS GRITS, SANDS AND CLAYS
CRETACEOUS		CLAY, SHALE, COAL, SANDSTONE AND LIMESTONE, etc.
JURASSIC	YOUNGER GRANITES	GRANITE SYENITES AND GABBRO
PRE-CAMBRIAN TO UPPER CAMBRIAN	BASEMENT COMPLEX	OLDER GRANITES UNDIFFERENTIATED BASEMENT COMPLEX

Fig. 2.1. Geological map of Upper Benue



LEGEND

Quaternary — Chad Formation

Tertiary — Basalts; Kerri Kerri Formation

F — F' Fault approximation

Antictinal axis

Synclinal axis

Cretaceous — Gombe Sandstone; Pindiga Formation; Bima Sandstone

Precambrian & Uppercambrian — Basement Complex

Fig. 2.2. Geological map of the study area, (after Cotter et al., 1963)

schists, biotite and hornblende, and granulites. After at least two tectonometamorphic cycles and consequent metamorphism, migmatisation and granitisation, the original rocks have been extensively modified so that they generally occur as relic rafts and xenoliths in migmatites and granites. The metasediments recognised within the Basement Complex are believed to be relics of an old supracrustal cover of probable Birrimian age and are termed Older Metasediments.

The Younger Metaseimdnets are believed to be Katangan in age. It is believed that they once covered the whole basement area having been removed by subsequent erosion so that they are now preserved in synclinal troughs. The metasediments include phyllites, schists, quartzites and conglomerates (Carter et al., 1963).

The Older Granite series include rocks intruded during the Pan-African orogenic cycle (Carter et al., 1963) These are the basic and intermediate plutonic rocks, fine-grained granites and syntectonic granites.

2.3 Cretaceous

Two major depositional basins, the Benue Basin and the Chad Basin, existed in this area of Nigeria during the Upper Cretaceous times. These are separated by the

Zambuk ridge which runs roughly north-eastwards from Gombe town to Biu Plateau (Carter et al., 1963). The depositions of sediments started during the Middle Albian (Lower Cretaceous) and ended about the Maestrichtian. The stratigraphical sequence in the Upper Benue Trough is given in Table 2.1 The formations represented in the study area include, Bima sandstones, Pindiga formation and Gombe sandstones.

The Bima sandstones are at the base of the sedimentary succession overlaying the basement complex. It is a basal continental sequence of argillaceous rocks and coarse grained sandstones (Carter et al., 1963).

The Pindiga formation is a sequence of marine shales which include a number of limestones towards the base. This formation approximately corresponds to Dukul, Jessu, Sekule formation and Numanha shales of the Benue Basin (See Table 2.1).

The Gombe sandstones is a sequence of estuarine and deltaic sandstone, siltstones, shales and ironstones which overlie the sediments of the Zambuk ridge and the Chad Basin.

2.4 Tertiary and Quaternary

After a period of folding a sequence of sediments was unconformably overlain on the continental Maestrichtian along the southern margin of the Chad

TABLE 2.1: General Stratigraphical Succession in the Upper Benue Trough

AGE	GEOLOGICAL TIME		UPPER BENUE BASIN: LAU	ZAMBUK-GULANI	GOMBE
Paleocence					Kerri-Kerri Fm.
CRETACEOUS	MAESTRICHTIAN		Lamja sst		
	SENONIAN	Campanian	Numanha Shales	Gulani sst.	Pindiga Formation
		Santonian	Sekule Fm.		
		Coniacian			
	TURONIAN	Upper	Jessu Fm.		
		Middle			
		Lower	Dukul Fm.		
	CENOMANIAN		Yolde Fm.		Yolde Fm.
	MID-LATE ALBIAN		Bima sst.	Bima sst.	Bima sst.
Late Palaeozoic to Pre-Cambrian			BASEMENT COMPLEX		

Stratigraphy: Compiled from (Carter et al., 1963; Cratchley and Jones, 1965; Wright, 1976; Offodile, 1976; Kogbe, 1981a).

Basin during the Tertiary and Quarternary.

The Tertiary sedimentary rocks consists of a continental sequence of flat-lying grits, standstones and clays termed the Kerri-Kerri formation. This formation underlies the Kerri-Kerri Plateau, the high plains near Fika, Potiskum and extends southwards beyond Gongola River to Gombe, Its age is Paleocene (Cartar et al. 1963)

The Quarternary sedimentary rocks are assigned to the Chad formation. It is a sequence of lacustrine fluviatile clays and sands of Pleistocene age. The Chad formation dips gently eastwards toward the centre of the Chad Basin.

2.5 Volcanic Activities

Volcanic rocks are widely distributed in the north-eastern part of Nigeria. The youngest and more important phase of activity occured during the Mid-Tertiary to Recent times. There is also evidence of volcanic activity during the Cretaceous.

The volcanic activity that occurred throughout the Upper Cretaceous volcanics are present on the Zambuk ridge of Kuman and Pandan hill. These consist of thin lavas and tufts which are thin, poorly exposed and deeply weathered for detailed study (Carter et al., 1963).

The volcanic actively which occurred in the Late Tertiary and Quanternary resulted in emplacement of volcanic plugs and the great lava plateaux of Biu and Longuda. A majority of the plugs are composed of fine-grained olivine-basalt, although a few are trachytic and phonolitic in composition. They intrude all the formations of the Cretaceous succession except the Kerri-Kerri formation or later rocks. The Biu Plateau is capped by sheets of olivine-basalts and runs southwards from Ligda through Bularaba and Balbaya to the north of Kwaya Terra (Fig. 2.2) where it swings to the east. In Biu the basalts are known to attain a thickness of 240m but in other areas its thickness is less than 30m (Carter et al, 1963).

2.6 Structures

In this region the sturctures have been largely determined by earth movements of late Cretaceous age. The movement ceased before the Tertiary. Thus the Paleocene and younger strata are flat-lying and unaffected by folding and faulting (Carter et al., 1963) The crystalline basement which is chiefly comprised of Older Granites has not indicated any structural pattern to show evidence of Precambrian earth movements. The main structure in this area are faults and folds. The faulting FF' is later than the folding and has affected all the Cretaceous rocks. The

chief fold elements as mapped by Carter et al., (1963) include the Gulani syncline as' and Dumbulwa anticline aa'.

CHAPTER 3

AEROMAGNETIC METHOD OF INTERPRETATION

3.1 Introduction to Aeromagnetic Method

The airborne magnetometer which was developed during the second World War for tracking submerged submarines combined with radio-location or other means for accurately locating the airplane, constitutes a new method of modern geophysics by means of which magnetic surveys are made with speed over land or water (Vacquier et al. 1951). The earth's magnetic field is mapped to guide our speculation with regards to the structure of the portion of the earth's crust which contains reasonable amount of ferromagnetic minerals. The crystalline rocks of igneous origin, such as granite, basalt and gabbro contain some appreciable amount of ferromagnetic minerals such as magnetite or haematite. The rocks thus have a weak magnetization which is likely to be induced by the earth's magnetic field and is in part permanent or remanent. This magnetization influences the earth's magnetic field above the surface of the earth to an extent that can be detected by sensitive instruments. The use of the aeromagnetic method in basement mapping to determine the maximum depth of sedimentation in geologic basin lies in the fact that sedimentary rocks are practically non-magnetic, whereas igneous and metamorphic rocks are, to varying degrees magnetic depending on their mineral composition. These rocks probably lose their

ferromagnetic properties at some depths where their temperature rises above the Curie point which is between 18 Km-27 Km (Ofoegbu, 1985). The anomalies in the earth's magnetic field with which we are concerned originate in that portion of the earth's crust which extends from this depth to the top of the crystalline basement complex.

The instruments adapted for use in airborne work include the flux-gate, nuclear precession and optical pump magnetometer. Virtually all airborne detecting systems measure total fields (Dobrin 1976, Telford et al., 1976).

To remove magnetic effects of the airplane, several arrangements are used in mounting the magnetometer. One way is to tow the sensing element at the end of the cable about 25 m-30 m long. Thus the detector housed in a streamlined cylindrical container known as the "bird", is usually nearer the ground than the aircraft with sufficient altitude maintained to prevent fouling it in tree tops.

Another problem in airborne surveying is to locate the aircraft at all times with respect to ground position. Techniques used in this respect include radio devices, aerial photography and doppler system of navigation. Details of these methods may be found in

many geophysical texts like Dobrin (1976) and Telford et al. (1976).

Although the speed of an airborne magnetic survey reduces the importance of instrumental drift and the diurnal magnetic variation, it is still necessary to correct for these effects. This is usually done by flying along parallel lines tied together by cross lines at an interval of several times the primary line spacing such that the survey lines and cross lines form closed loops around which the magnetic changes may be adjusted for closure (Griffith and King 1965, Nettleton, 1971). Another method of removing non-closure at cross over points, is given by Mittal (1984).

The data of a magnetic survey are presented on contour maps showing lines of equal strength of the anomaly field or any of its components. The areal extent of the features roughly represents the extent of contrast in average content of ferromagnetic minerals of the underlying basement rock.

The first step in the interpretation of aeromagnetic maps is qualitative, with the aim of detecting such charateristics as anomaly distribution, structural trends, etc. However, the information that can be deduced from a survey is considerably increased if some geological information is already available. Many methods are available for the purpose of quantitative interpretation. These include

curve-fitting methods based on a few specified points of a magnetic profile, upward or downwards continuation, among others (Peters, 1949; Vacquier et al 1951; Werner, 1953; Hutchison, 1958; Gay, 1963; Naidu 1969).

The interpretation method used in this study operates on the measured fields and the horizontal derivative. It is an extension of the technique introduced by Werner (1953) and discussed in the next section.

3.2 The Werner Deconvolution Technique

The Werner deconvolution technique was first introduced by Werner in 1953. It is a method of direct interpretation to determine the depth, magnetic susceptibility and dip of semi-infinite homogenous, thin sheets, whatever their strike, dip or remanent magnetization and at any magnetic latitude (Hartman et al., 1971). The method allows for the separation of an anomaly from interference caused by adjoining anomalies. Werner was mainly concerned with the analysis of mineralized dykes in Sweden, and his paper was written for the identification of thin dykes. The method was later shown to be applicable to contacts, edges, faults and other types of bodies (Hartman et al., 1971, Friedberg, 1975; Jain, 1976; Ku and Sharp, 1983).

3.2.1 Mathematical Derivation

The following derivations are based on the concept of magnetic charge or pole-strength as described by Gay (1963). Consider a homogeneously magnetized thin dyke with infinite strike length, extending to infinite depth and with parallel sides in a left-handed coordinate system (Fig. 3.1). The symbols used to further describe the dimension, position, sheet magnetization and magnetizing field are defined below (see also Fig. 3.2).

t = thickness of sheet.

δ = dip angle of sheet. This is the angle between the positive y-axis and the plane of the dyke.

α = the magnetic strike. It is the clockwise angle from the magnetic north to the strike direction of dyke.

k = magnetic susceptibility contrast between the dyke and the surrounding material.

T_o = Magnitude of the earth's total magnetic field.

I_o = Inclination of the earth's field in the yz plane.

T_s = a component of the total field parallel to the x' - axis. It is neglected since any magnetic poles it induces on the end faces are at infinity.

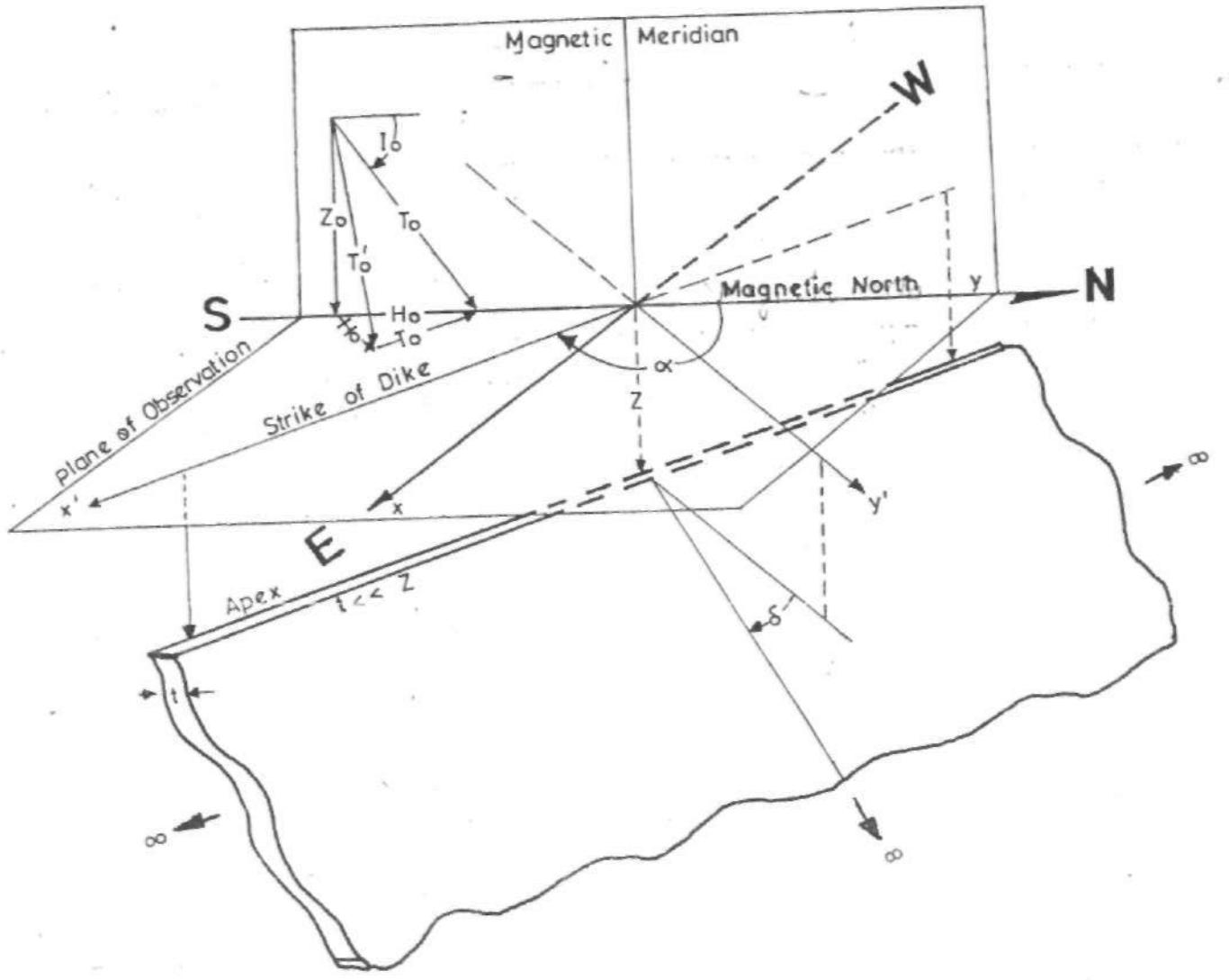


Fig. 3.1. Geometry and spatial relation of thin infinite dyke (after Gay, 1963)

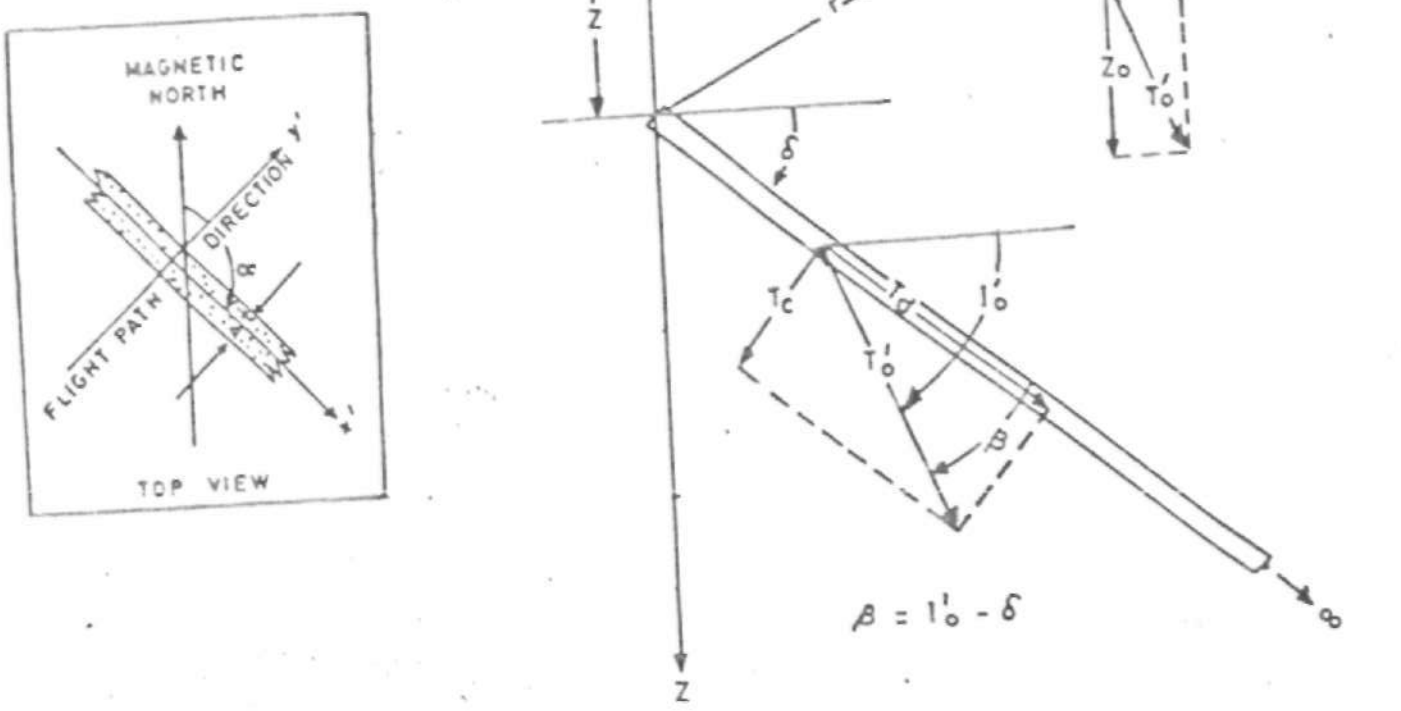


Fig. 3.2. Geometry of thin dyke: (A) top view and (B) cross sectional view

T_o' = the other component of the field effective in inducing magnetic poles on the dyke's surface.

I_o' = the effective inclination. It is the inclination of T_o' in the y'z plane.

T_d = the component of the effective magnetic field parallel to the dip of the dyke.

T_c = The component of the effective magnetization perpendicular to the plane of the dyke.

The dip component (T_d) and cross-component (T_c) of the inducing field create corresponding components of internal magnetization in the dyke. The dip component induces a narrow strip of charge of magnetic pole-strength per unit area, M_d where

$$M_d = KT_d \qquad \text{.....(1)}$$

Also the cross-component induces on the upper and lower surfaces a magnetic pole-strength per unit area, M_c given by:

$$M_c = KT_c \qquad \text{.....(2)}$$

The expressions for M_d and M_c hold only when demagnetization effects are neglected. The magnetic anomaly is derived from the potential due to these distributed magnetic poles. At a point on the plane of observations the long linear distribution of poles on the apical edge gives rise to the logarithmic potential

given in Gay (1963) as:

$$V_d = 2KT_d t \log (y'+z^2)^{-1/2} \qquad \ldots\ldots\ldots (3)$$

On the planer surface of the dyke, T_c induces two closely spaced sheets of magnetic charge of opposite signs. The potential due to this is given in Gay (1963) as

$$V_c = 2KT_c t\ (90^o - d + \tan^{-1} y'/z) \qquad \ldots\ldots\ldots (4)$$

By adding (3) and (4) and taking the proper derivatives, the vertical and horizontal intensity anomalies may be derived as

$$\Delta Z = -\frac{dv}{dz} = \frac{2t\ (M_d z + M_c y')}{z^2 + y'^2} \qquad \ldots\ldots\ldots (5)$$

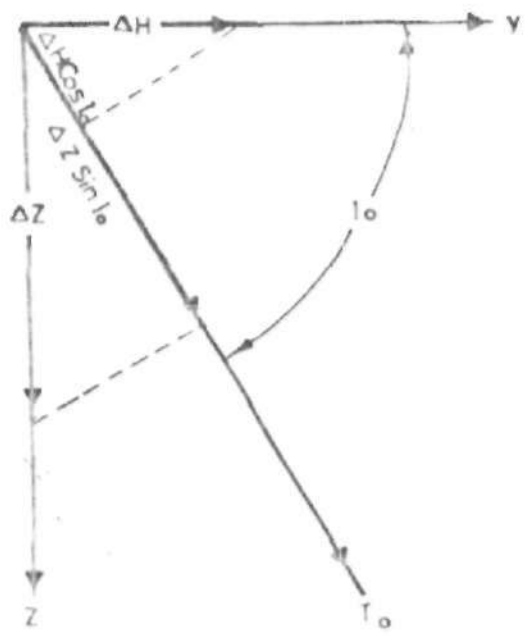
$$\Delta H' = \frac{dv}{dy'} = \frac{-2t(M_d y' - M_c z)}{z^2 + y'^2} \qquad \ldots\ldots\ldots (6)$$

Where H' is the anomly in the component of the horizontal intensity in the direction of y'. The component in the direction of magnetic north is commonly measured and is given by

$$\Delta H = \Delta H' \sin\alpha \qquad \ldots\ldots\ldots (7)$$

It can be shown (Fig. 3.3) that F, the anomaly in the direction of the total Intensity i.e. in the direction of T_o, the undisturbed field, is given by

$$F = \Delta Z \sin I_o + \Delta H' \cos I_o \sin\alpha \qquad \ldots\ldots\ldots (8)$$



$$F = \Delta Z \sin I_o + \Delta H \cos I_o$$

FIG 3.3 RELATIONSHIP BETWEEN
THE TOTAL FIELD AND ITS
COMPONENTS IN Y-Z PLANE

and using (5) and (6)

$$F = \frac{Ay' + Bz}{z^2 + y'^2} \qquad \text{.....(9)}$$

where

$$A = 2t(M_c \sin I_o - M_d \cos I_o \sin\alpha) \qquad \text{.....(9a)}$$

$$B = 2t(M_d \sin I_o + M_c \cos I_o \sin\alpha) \qquad \text{.....(9b)}$$

Solving (9a) and (9b) we can write

$$M_c = \frac{A \sin I_o + \cos I_o \cos\alpha}{2t(\sin^2 I_o + \cos^2 I_o \sin^2\alpha)} \qquad \text{.....(9c)}$$

and

$$M_d = \frac{A \cos I_o \sin\alpha + B \sin I_o}{2t(\sin^2 I_o + \cos^2 I_o \sin^2\alpha)} \qquad \text{.....(9d)}$$

Equation (9) is the basic equation used in Werner deconvolution of total field data. It is an expression for the total field in terms of the interpretation parameters when the centre of the dyke body (Fig. 3.2) is located at (0,z). For an arbitrarily horizontal location at (y',Z) equation (9) becomes:

$$F = \frac{A(y' - y_o') + Bz}{(y' - y_o')^2 + z^2} \qquad \text{.....(10)}$$

Werner (1953)in his interpretation considered the effect of interference in the anomalous field. Some of the factors that could result in such interference

were enumerated by Jain(1976)as:

1) The magnetic field due to deep-seated bodies, commonly called regional anomalies or anomalies due to shallow bodies located at large lateral distances away.

2) anomalies due to a sheet of limited extent laterally or vertically.

3) the presence of local magnetic masses or observational errors, which affect a small area and then rapidly become insignificant.

The interference field is represented by a polynomial of some degree which is then added to equation (10). In this study a second degree polynomial was used in agreement with Jain (1976). Also Kilty (1983) noted that fitting higher order polynomials makes the residual susceptible to noise. The assumption of a second degree polynomial yields:

$$F = \frac{A(y'-y'_o)+Bz}{(y'-y'_o)^2+z^2} + C_o + C_1 y' + C_2 y'^2 \quad \ldots\ldots(11)$$

Equation (11) can be written in the form

$$a_o+a_1y'+a_2y'^2+a_3y'^3+a_4y'^4+b_oF+b_1y'F=y'^2F \quad \ldots\ldots\ldots\ldots(12)$$

where

$$a_o = -Ay'_o + Bz + C_oz^2 + y'^2_oC_o$$

$$a_1 = A-2C_oy'_o + y'^2_oC_1 + C_1z^2$$

$$a_2 = C_o-2C_1y'_o + C_2y'^2_o + C_2z^2 \quad \ldots\ldots\ldots\ldots(13)$$

$$a_3 = C_1 - 2y'_oC_2$$

$$a_4 = C_2$$

$$b_o = -y'^2_o - z^2$$

and

$b_1 = 2y_o'$

This is a linear equation with seven unknowns. If the values of F at seven data points are known it should be possible to obtain the values of the unknown parameters simply by solving seven simultaneous linear equations. In practice an equally spaced seven-point operator, with the fourth point of the operator as the reference is used. Finally the following results for a thin dyke in real physical dimension are obtained in terms of the sample spacing $\Delta y'$ (Ku and sharp, 1983):

Horizontal position $(x_o) = 0.5b_1y' + \Delta y'$ .....(14)

Depth $(Z) = (-b_o - 0.25b_1^2)^{1/2} \Delta y'$ .....(14b)

Magnetic susceptibility contrast (K) is given by

$K = (T_o') (M_d^2 + M_c^2)^{1/2} \Delta y' / |T_o'|$ .....(14c)

and

Dip (d) = $\tan^{-1} (\tan I_o'/\sin\alpha - \tan^{-1}(M_c/M_d)$.....(14d)

where $\tan I_o' = \tan I_o/\sin\alpha$ and

$T_o' = T_o \sin I_o/\sin I_o'$ (see fig. 3.2)

The theory developed above is valid at any magnetic latitude for all semi-infinite homogeneous, sheet-like bodies with any strike and dip. If the derivative of the total field is taken, the differentiation and integration cancel. This implies that the magnetic anomaly for a thin sheet is the same as the derivative of the magnetic anomaly for a similarly positioned interface. The derivative used in

this paper is the horizontal gradient. In digital form the horizontal gradient is calculated from the total field using the Lagrangian interpolation (Ku and Sharp, 1983). The same set of equations used for total field interpretation is also used for horizontal gradient interpretation. Thus, it is possible to compute the horizontal gradient from the total field and use the same equation to estimate the source parameters for an edge.

3.3 Method of Application of Werner Deconvolution.

Usually, measurements of the magnetic field are made at equal linear intervals along profiles. Therefore the data are in the ideal form for digital analysis. A computer program written by Dr. S.B. Ojo of the Physics Department, A.B.U., Zaria was used. The program interpretes equally spaced profile data using equations (12) through (14). It reads six equally spaced points along a profile (for the case in which the interference field is represented by a first degree polynomial) or seven equally spaced point (for second degree polynomial interference field. The window of six or seven points (operator) is moved along the profile at one point interval and the parameters of equation (14) computed at each point. If the Werner operator is of a size comparable to the size of an anomaly a group of solutions is obtained when the operator straddles the anomaly. The variation in

solution may be so large that some of the solutions may need to be discarded. To reduce the number of these stray depth interpretation, the depth estimate of neighbouring points are assumed to originate from the same source when (a) the locations (x_o of equation 14) for the group of points are equal within a certain specified value usually about half the sample interval, and (b) the depths are within 10 per cent of one another for the group of points. The number of estimates in a group is used as a weighting factor in interpretation.

The detection of an anomalous source is related to the size of the operator window. A deep source with an associated broad magnetic anomaly needs a Werner operator of comparable size to recognise it. For this reason the size of the operator is varied by increasing the interval of points used and the computation sequence earlier described repeated. The original data are smoothed with a low pass Hamming window before each pass of the operator to prevent aliasing effects caused by the increased interval. This filtered data produces a broader anomaly of lower amplitude which is then interpreted as arising from a deeper source. This results in a vertical array of depth points over several hundred meters. In such a case, the correct depth is near the top of the vertical array of depth points

If thin dykes are present, their anomalies are recognised and analysed from the total field data, while interfaces are analysed from the computed horizontal gradient of the total field. Because of certain mathematical similarities between the total field and its horizontal gradient, most anomalies yield both gradient and total field depths.

One of the physical implications of these derived equations is that when the Werner operator is small compared with the anomaly size, the operator will see only a small or nearly linear part of the anomaly with resultant depth solutions deeper than the true depth. On the other hand, if the operator size is too large, it would likely see multiple peaks from adjacent anomalies, thus resulting in erroneous calculations. The desirable operator size should actually be from one-half to full size of the magnetic anomaly under deconvolution (Ku and Sharp, 1983).

Another physical implication of the equations is that, to determine the true magnetic susceptibility one must know the thickness of the dyke, and vice versa.

Finally it should be noted that though the equations have been derived from a vertical dyke, it is generally valid for a dyke dipping at any angle, so long as the dyke is thin in comparision to its depth.

3.3.1 Results from theoretical model studies

To test the validity of Werner deconvolution

method, model studies of geologic bodies varying from thin dykes to the edge of thick interface and low basement topographic relief have been carried out by many workers (Hartman, et al., 1971; Friedberg, 1975; Jain, 1976). In this section deconvolution is applied to a basin model as a means of testing the reliability of the same computer program before its application in this study. Another computer program (Ojo, Personal Communication) was used to generate the total field intensity due to a two dimensional basin model. Deconvolution was then applied to the total field and the generated depths plotted. The result is summarised in Fig. 3.4

The results show that the computer program identified changes of slope satisfactorily. It was also noticed that as with other studies (Hartman et al., 1971; Friedberg, 1975) the horizontal field solutions gave depths shallower than the total field solution. Also the generated depths lie either exactly or very close to the model depths. This factor was found very useful in the interpretation of real data where the interpreted depths were considered to be represented by the minimum depth within a group of depths. It is considered that this will introduce an error of about 10 percent in agreement with Hartman, et al., (1971) and Friedberg, (1975). However when very shallow depths less than 0.7 Km(about half the length of the smallest Werner operator) are used the error could be

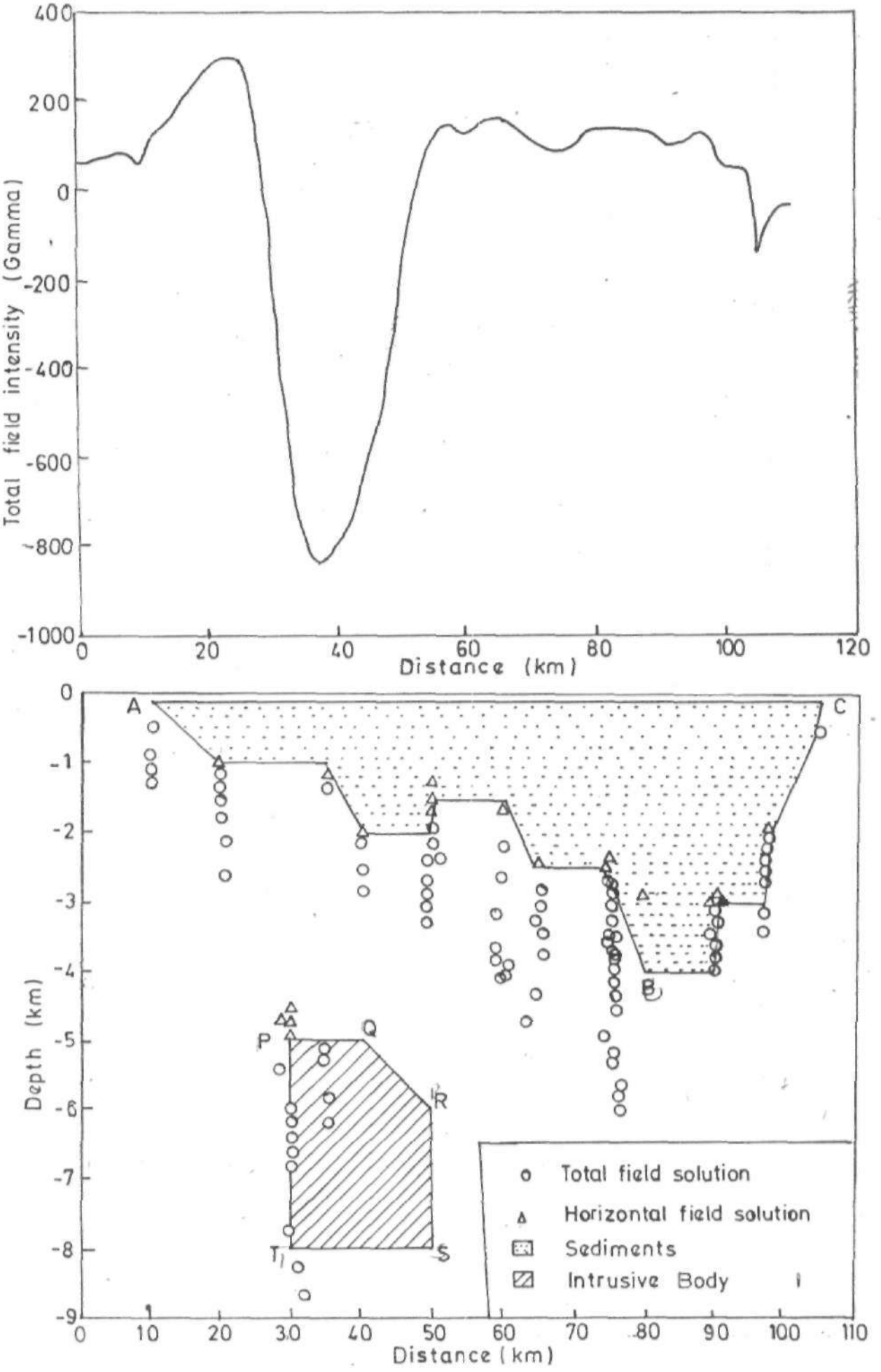


Fig. 3.4. Interpretation of a theoretical basin model using Werner deconvolution method.

more than 10 percent as seen in position A and C in Fig. 3.4 Position B in the same figure is not identified at all. This shows that not all basement features are likly to be recognised using this method. When intrusives like PQRST are present, it is shown that they could be effectively masked by shallower features.

CHAPTER 4

RESULTS AND INTERPRETATION

4.1 Introduction

The interpretation is divided into qualitative and quantitative interpretation. In the qualitative interpretation effort is made to describe the aeromagnetic field pattern of the study areas and relate it to the known geology. The quantitative interpretation covers the analysis of magnetic anomalies along profiles drawn as close as possible to flight lines. The aeromagnetic data used was in the form of contoured 1:100,000 aeromagnetic maps. These were compiled in 1975 by the Geologic Survey of Nigeria. The regional correction on the aeromagnetic data was based on the International Geomagnetic Reference Field (IGRF) epoch date, 1st January, 1976. The flight parameters of the map is given in table 4.1

4.2 Qualitative Interpretation

An aeromagnetic map is essentially a reflection of the contrast between the magnetic properties of rocks over which the measurements were carried out. Thus the magnetic expression of such features depend on the strength of the magnetic contrast in the body of the rocks involved. The character and composition of rocks control the distinctness with which they are expressed on aeromagnetic maps (Domzalski, 1966). To aid the interpretation, the aeromagnetic map and geological

TABLE 4.1: FLIGHT PARAMETERS

Flight direction.....150° /330°

Tie line direction .....60°/240°

Nominal flight spacing .....2 Km

Nominal tie line spacing .....20 Km

Nominal flying altitude above terrain ...0.15 Km

maps were reduced to the same scale convenient for easy correlation. Fig. 4.1 shows the essential features of the aeromagnetic map of the areas.

A careful study of this map shows two distinct anomaly pattern and these have been demarcated by the line AB on the map. To the east of line AB is a complicated distribution of short wavelength anomalies, while the rest of the map is marked by a relatively long wavelength anomaly pattern. Moreover the smaller widths of the anomalies in the eastern section as opposed to those on the western section of AB indicates that the magnetic sources to the east are generally shallower than in the other areas. Another distinct feature in the aeromagnetic map is the trend of the anomalies which is approximatly NE-SW with a few anomalies trending E-W. The anomalies are more or less elliptical in shape suggesting the presence of intrusive bodies alligned NE-SW and E-W. The most prominent NE-SW trending features are aligned along CC' suggesting the presence of lineament in this direction. Also there is an indication of a lineament LL' trending E.W. across the lower half of the study area.

4.2.1 Correlation of Aeromagnetic Anomalies with the known Geology.

Based on available geological information the study areas may be divided into two major regions - the

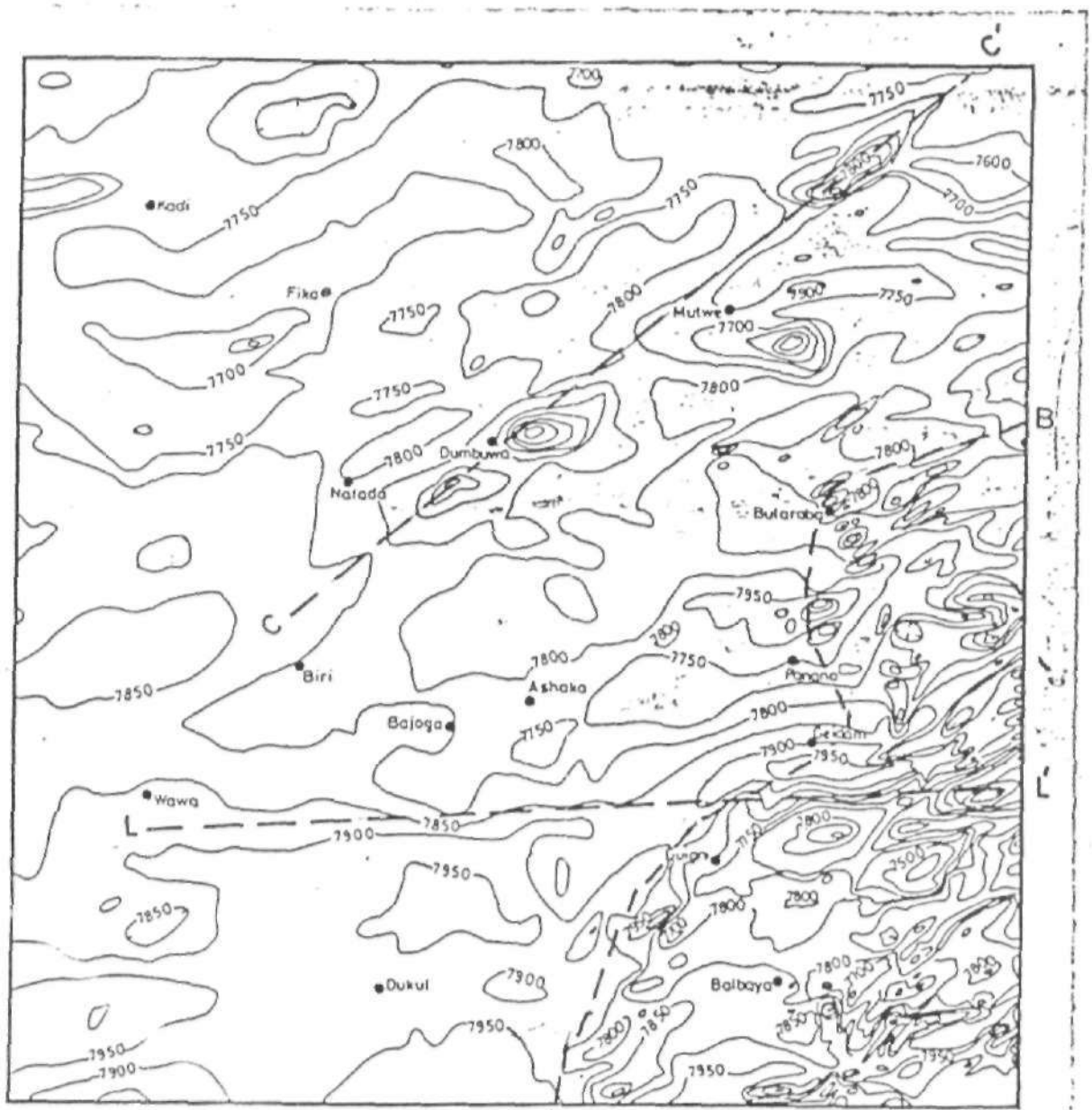
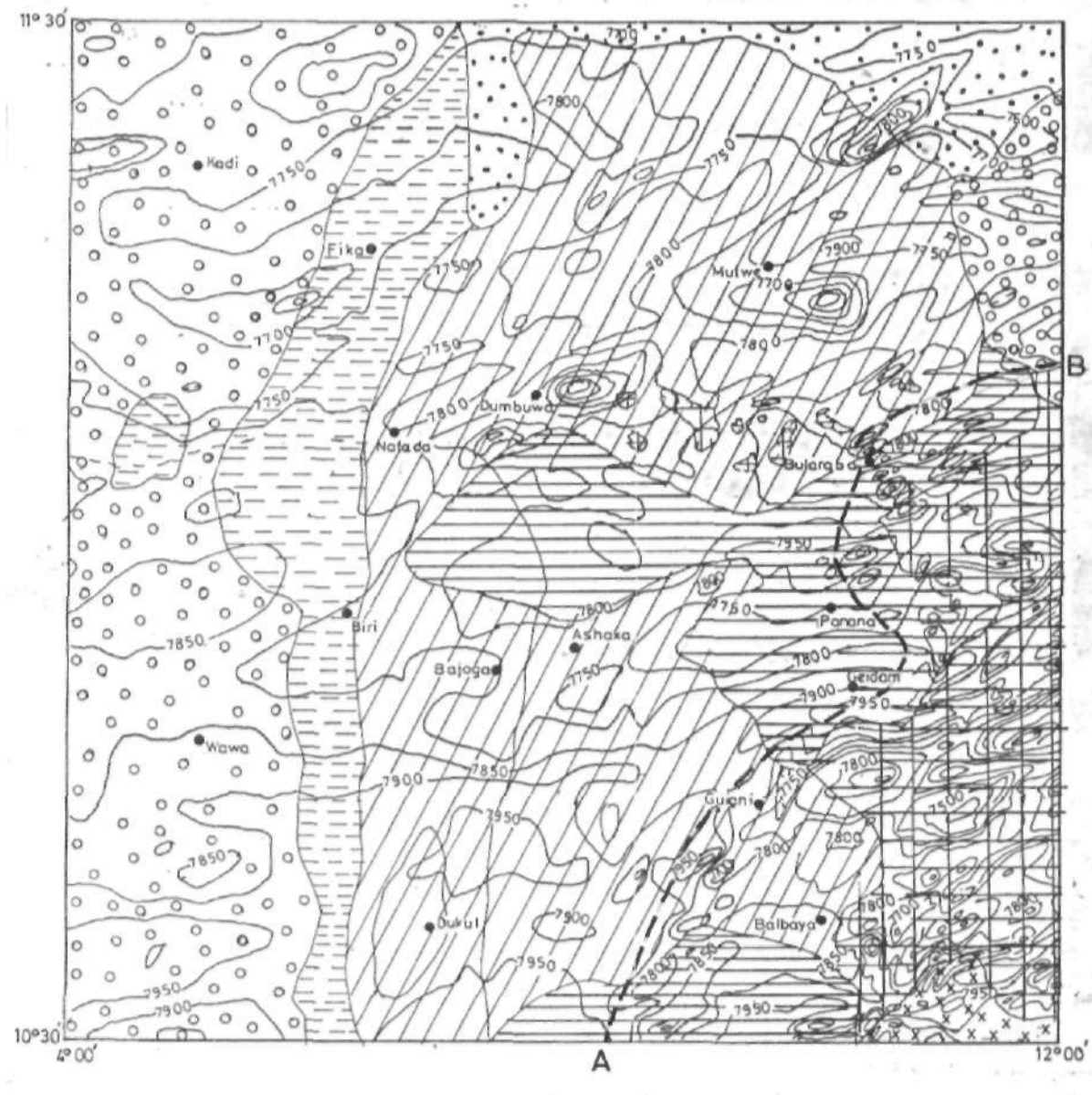


Fig. 4.1. Total magnetic field intensity of the study area. Contour interval is 50nT. To obtain the actual field values, add 25000nT to contour values. Line LL' and CC' are magnetic lineament; AB is a magnetic boundary.

extreme eastern section of the area marked by a few granitic instrusion surrounded by volcanic rocks; and the rest of the areas overlain by sedimentary rocks of different formation (Fig. 2.1).

Fig. 4.2 shows the aeromagnetic map superimposed on the geological map for the purpose of correlation between the two. It is apparent that two distinct zones shown on the geologic map are also recognisable on the aeromagnetic map. The area in the aeromagnetic map with smooth contours and low magnetic relief correlate well with the sedimentary section while the other areas with steep gradient and high magnetic relief correlates well with the basement outcrops and highly magnetic basaltic rocks of the Biu Plateau. It seems however, from the magnetic pattern that pockets of rocks or shallow basement may lie buried beneath the Cretaceous sediments as indicated by scattered, isolated anomalies over Bima and Pindiga formations. Many earlier workers have suggested the presence of intrusives at various depths up to 12 Km (Ajakaiye et al., 1986, Ofoegbu, 1984a • Ofoegbu (1985) also proposed that the anomalies over the trough could best be explained in terms of basement of varied topographic relief together with some basic or intermediate intrusions.

Finally the lineament shown by LL' and CC'(Fig.4.1) match some of the long, sub-parallel magnetic anomaly belts described by Ajakaiye et al., (1986). Both LL' and CC'



L E G E N D

Quarternary — Chad Formation

Tertiary — Basalts; Kerri Kerri Formation

Cretaceous — Gombe Sandstone; Pindiga Formation; Bima Sandstone

Precambrian & Uppercambrian — Basement Complex

Fig. 4.2. Combined geological and total field anomaly map. AB is a magnetic boundary.

cut across the Kerri-Kerri formation, Cretaceous formation and could be due to changes in the magnetic character of the underlying rocks or to structures such as faults or dykes.

4.3 Werner Deconvolution of Field Data.

The aeromagnetic map was digitized along straight profiles drawn along flight lines. The profiles are labelled by the flight line number (for example L120, L121, etc). The separation between adjacect profiles is about 2 Km. Aeromagnetic data is usually collected at interval of about 100 m. This is an ideal sampling interval for aeromagnetic interpretation. To avoid over interpolation of the already smoothened and in some cases low gradient magnetic data a sampling interval of 0.5 Km was used. The closeness of the profiles makes it possible for an anomaly to be crossed by more than one profile, thus making correlation of results from adjacent profiles possible. The computer program used is, in addition, able to reduce the digitizing interval to 0.25 Km using linear interpolation in order to reduce the smallest seven-point Werner operator to 1.5 Km wide. The input parameters, for the computer program are listed in table 4.2

Deconvolution was applied to fifty-one profiles in the study area. The operator lengths used vary from 1.5 Km to 22.5 Km in steps of 1.5 Km. This was adequate to fully interprete anomalies with widths varying from

TABLE 4.2 Input data for Werner deconolution

Title of profile	
Number of points in a profile	
Sampling interval	0.5 Km
Assumed average total field intensity	33000 nT
Angle of declination	0.0^{o}
Angle of inclination	4.5^{o}
Minimum number of consistent depth solution accepted (Weight)	3
Operator lengths used	1.5 Km - 22.5 Km

about 3 Km to about 40 Km and depth varying from about 0.7 Km to more than 11.0Km (Ku and Sharp, 1983). It is however not possible to interprete accurately very shallow magnetic basement regions or short wavelength field patterns because of the limitations imposed by the smoothed data and the fact that the smallest operator length 1.5 Km long, spans more than one anomaly resulting in erroneous calculations. The accepted depths from each profile were plotted to scale below the corresponding total field profile (see appendix). Plotted depths were compared with those of adjacent profiles which crossed the same anomaly. Generally, depths were not calculated along the first few kilometers from either ends of most profiles. This was because deconvolution was not started from the beginning of the profiles to avoid edge effect. Moreover most of the anomalies at either ends are not fully defined.

However there is enough information from the generated depths to correlate results from adjacent profiles. A careful study of some adjacent profiles shows that a magnetic basement surface can be fitted which is consistent for a set of profiles.

4.3.1 Profile Interpretations.

In this section results of Werner deconvolution would be examined to get such information as maximum thickness of sedimentary formation i.e. depth of

magnetic basement and presence of associated structures.

Fig. 4.3 shows interpretation of profiles L121, L121 and L123. The position of these profiles in relation to geologic map can be deduced from fig. 4.4. These profiles are short and do not yeild enough solution to enable a basement surface to be fitted. They are, however, used here to illustrate how adjacent profiles are correlated for consistency. The profiles are arranged so that magnetic field features, e.g. P corresponding to same anomalies are aligned. Solutions corresponding to these positions are compared for consistency. In this example, depths recorded for position P vary between 1.9 Km and 2.1 Km. Such consistent depths were noted for use in compilation of the basement depth map of the region. Figs 4.5 to Fig. 4.8 represent a set of profiles with similar magnetic features, yielding consistent Werner depths. By comparing calculated depths for adjacent profiles noting consistent depths it is possible to fit a magnetic basement surface that is representative for the group of profiles across the same anomalies. Such a surface gives a general idea of the depth to the magnetic features and hence the maximum thickness of the sediments. With the aid of such an interpreted surface it may be possible to deduce the presence of structures associated with the basement.

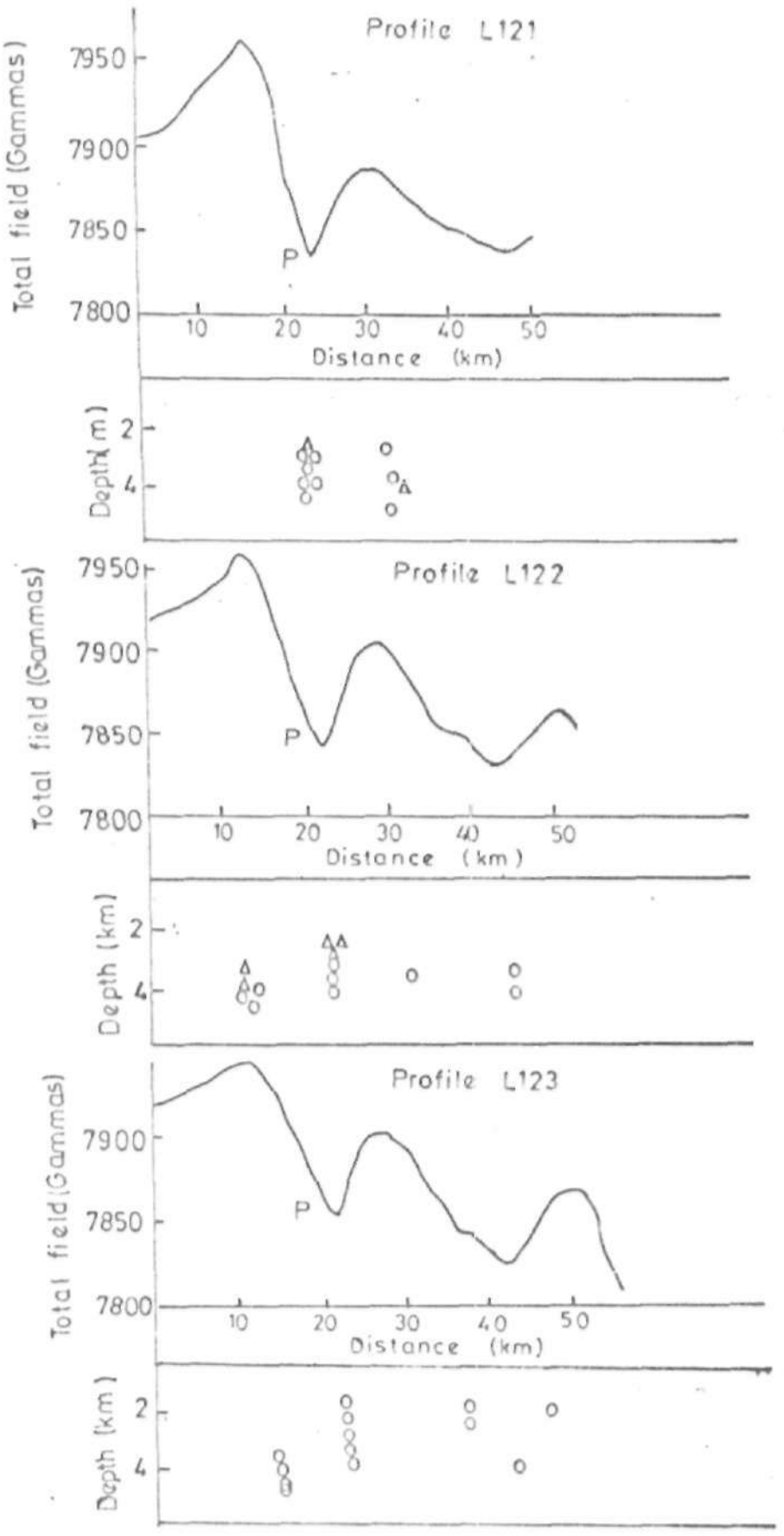
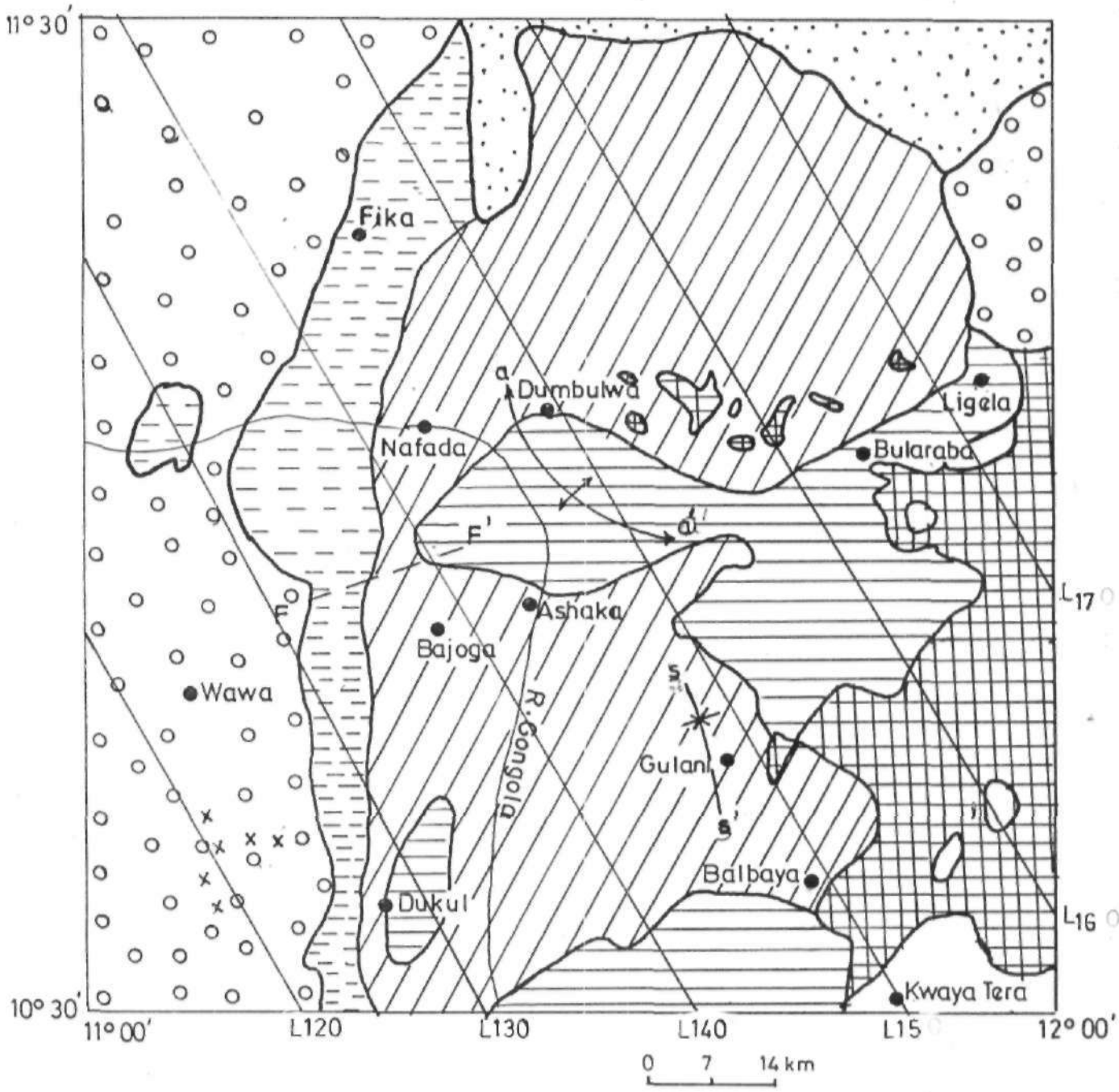


Fig. 4.3. Correlation of field profiles.



LEGEND

Quaternary — Chad Formation

Tertiary — Basalts; Kerri Kerri Formation

F — — F' Fault approximation

Antictinal axis

Synclinal axis

Cretaceous — Gombe Sandstone; Pindiga Formation; Bima Sandstone

Precambrian & Uppercambrian — Basement Complex

Fig. 4.4. Geological map showing position of slected field profiles

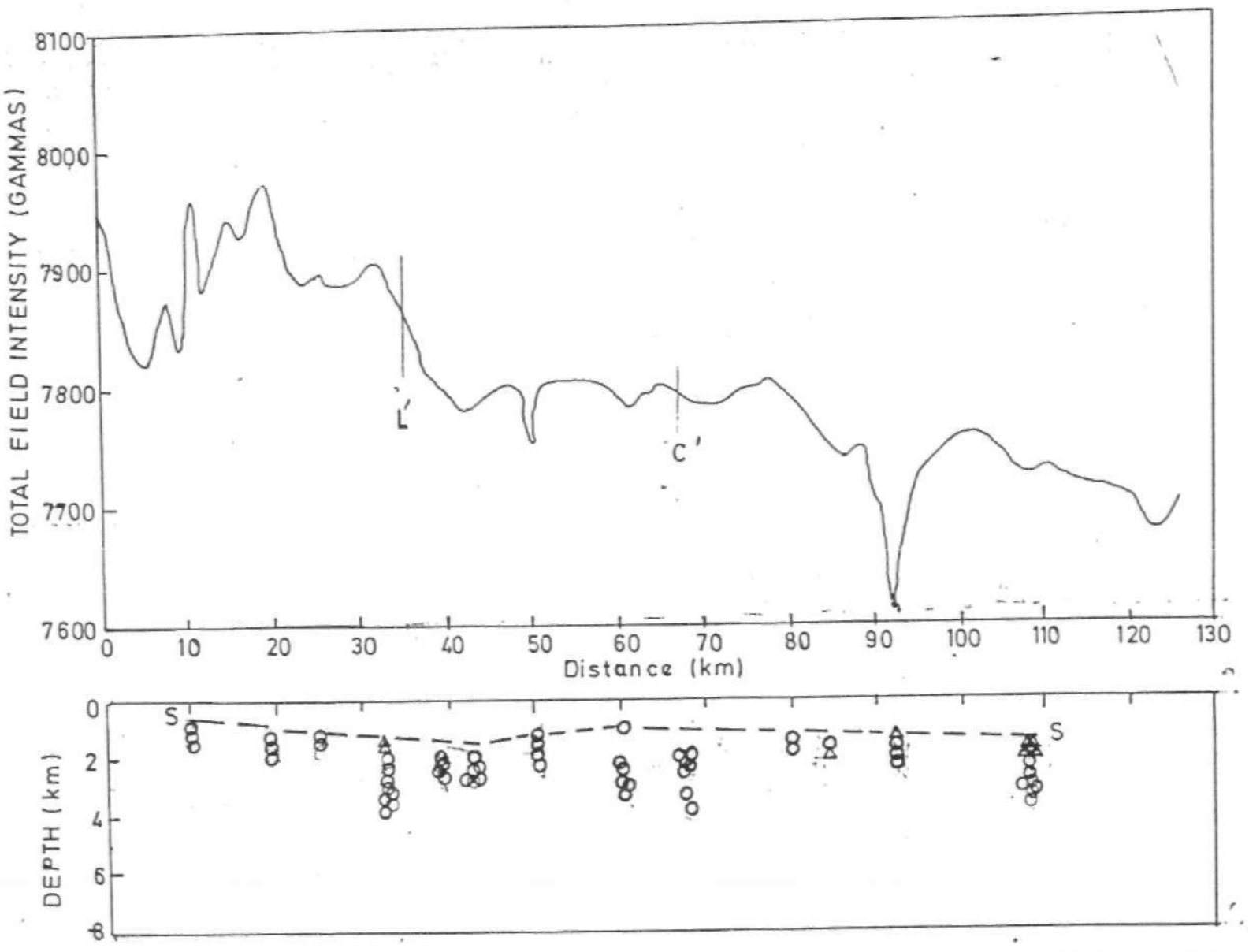


Fig. L 4.5. Interpretation of profiles L141 55' is the fitted magnetic basement surface

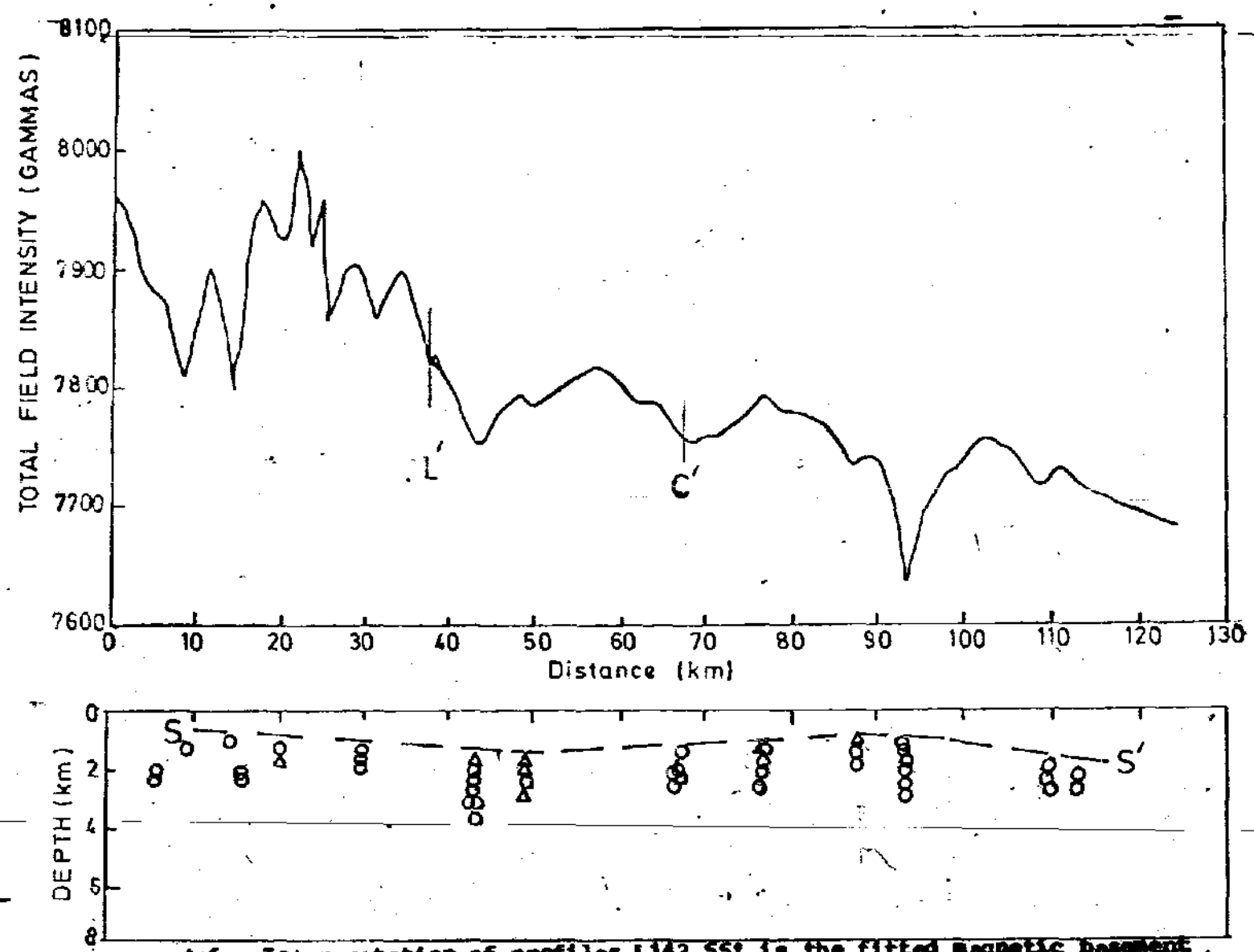


Fig. 4.6. Interpretation of profiles L142 55° is the fitted magnetic basement surface

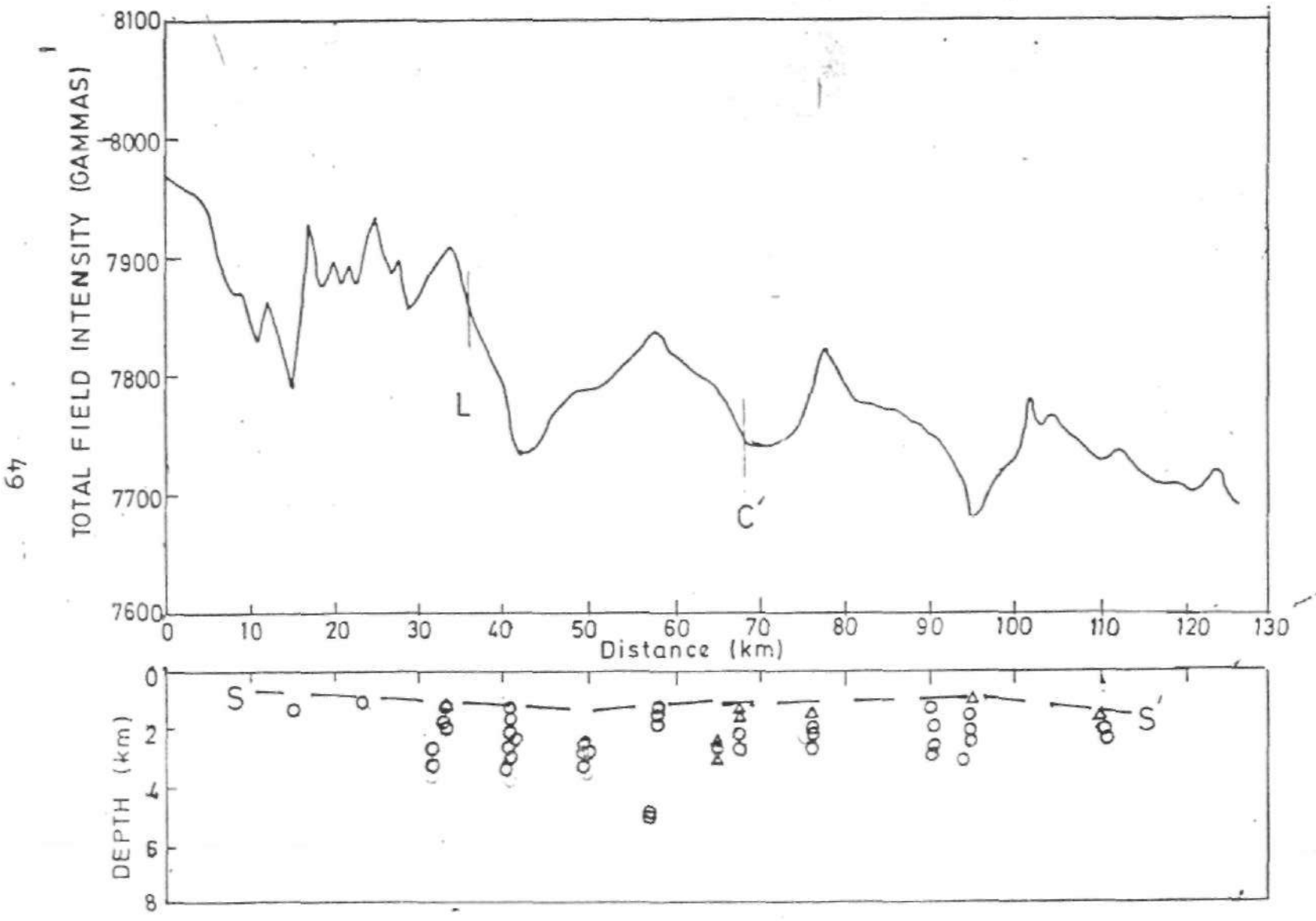


Fig. 4.7. Interpretation of profiles L143 SS' is the fitted magnetic basement surface.

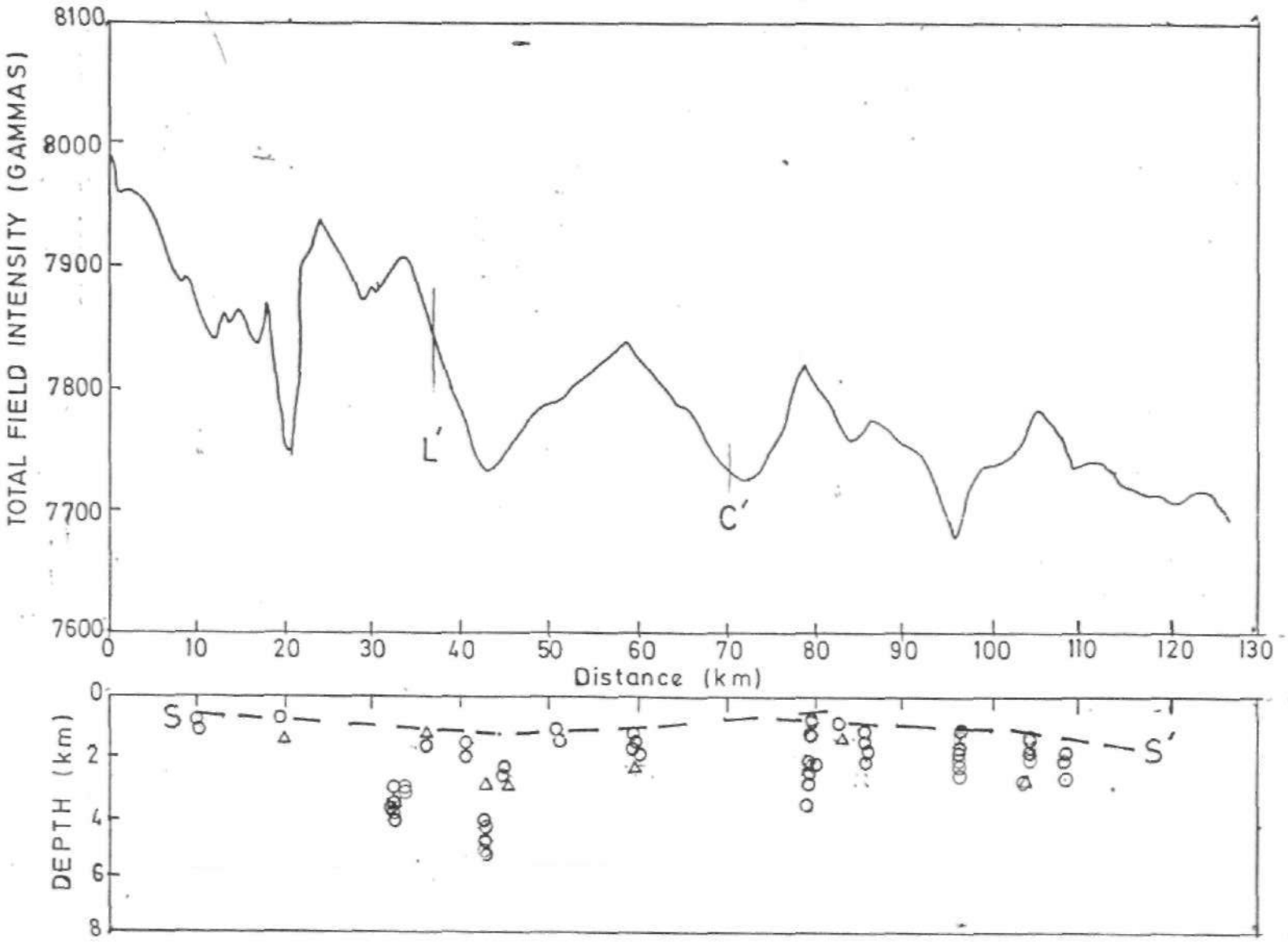


Fig. 4.8. Interpretation of profiles L144 SS' is the fitted magnetic basement surface.

The magnetic basement surface SS' fitted to the profiles is consistent for these set of profiles. The fitted surface shows that the maximum depth to the magnetic features and hence the maximum thickness of the sediments is between 1.4 Km and 2.0 Km. The surface SS' does not show the presence of either faults or folds which are usually associated with the Benue Trough. This does not imply that these structures are totally absent. The poor quality of the data could have led to poor resolution of magnetic features. On the other hand the orientation of these features in relation to the flight lines could also lead to the masking of such features. L' and C' in Fig 4.5 -Fig 4.8 show the position of lineament LL' and CC' in Fig 4.1. The interpreted magnetic basement shows that these lineaments could be due to variation in magnetization. This view is supported by the difference in magnetic signatures on either sides of L'.

There are however, profiles with very similar magnetic features yielding contrasting depths for corresponding anomaly positions on nearby profiles. In this group are profiles L129 and L130 in Fig. 4.9. Such profiles are not however, totally ignored in the interpretation since they sometimes provide depths which can be compared with depths of other profiles crossing the same anomalies. This lack of correlation

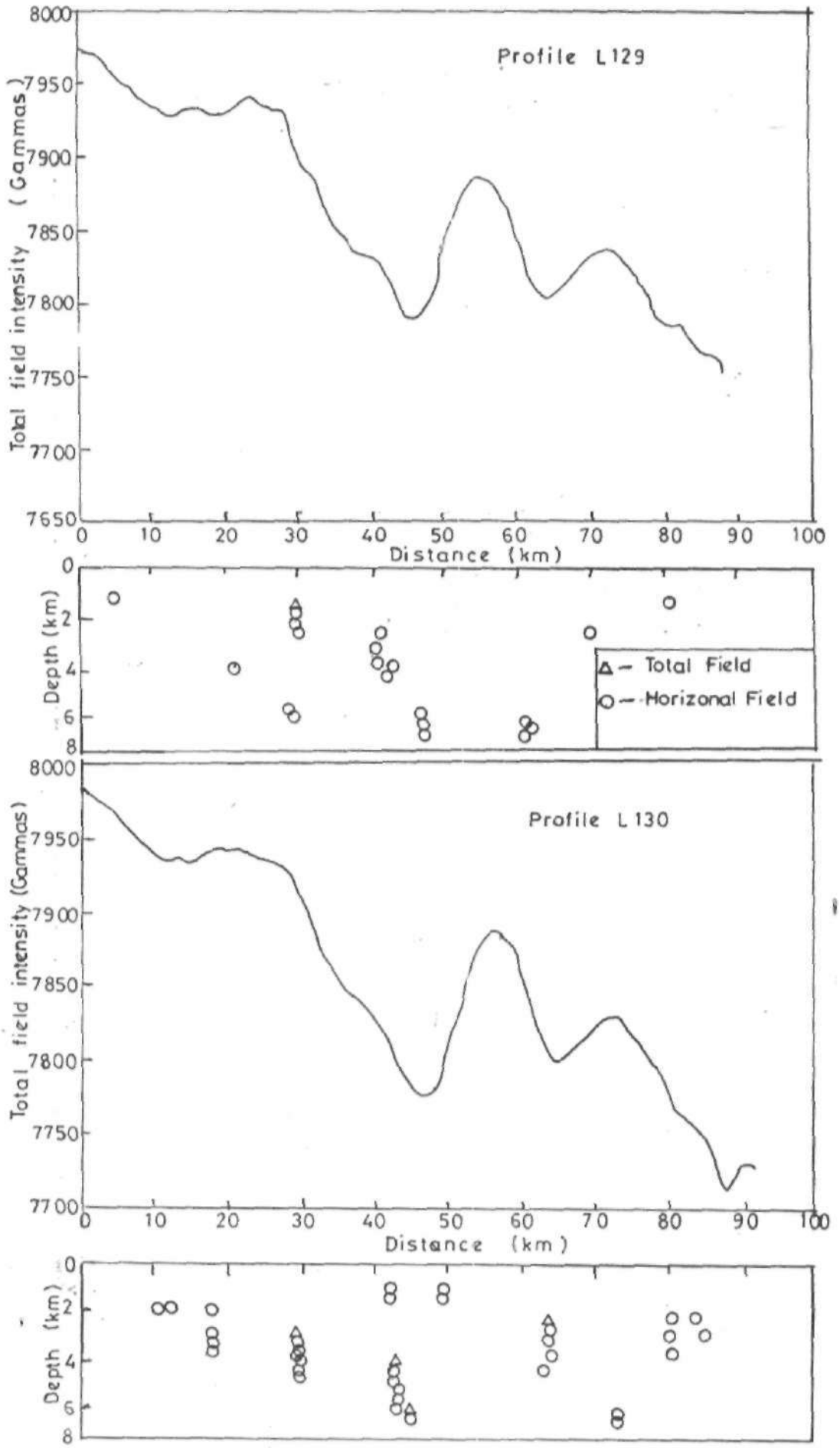
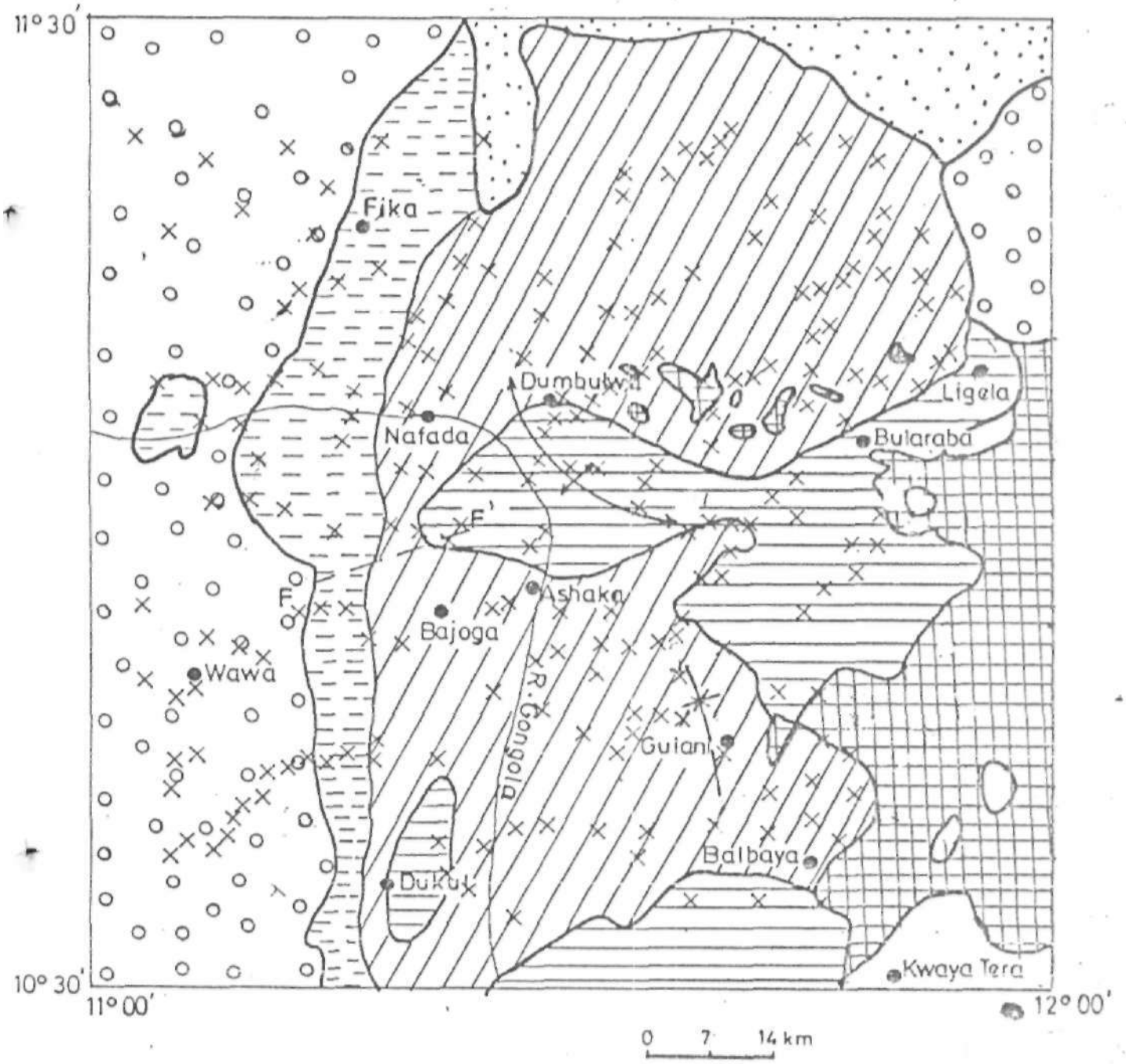


Fig. 4.9. Interpretation of profiles L129 and L 130. A case of uncorreleted depths for similar anomalies.

of results for similar magnetic features on adjacent profiles could be due to the fact that as a result of poor quality of the data, the features which could have shown up when small operator windows were used during deconvolution were masked in one profile but high-lighted in adjacent profiles. On the other hand, since the profiles are 2 Km apart differences in computed depths may actually represent lateral variation in depths of the sturctures.

4.4 Magnetic Basement Map.

The first step in preparing the basement map was to select acceptable depths from each profile and multiply each depth with the corresponding cosine correction factor. This is necessary in cases where the strike of the body as inferred from the magnetic map is not perpendicular to the profile line. The latitude and longitude of each accepted depth were recorded and used in the preparation of the map. The positions of the plotted depth points used are plotted in Fig. 4.10. The magnetic basement map superposed on the local geology of the area is shown in Fig. 4.11. The depth contour values are with respect to the flight elevation of 150m. The basement map shows that the depth varies from 1.4 Km to 2.0 Km with a general increase in depth from the east towards the west. The general relationship between the basement topography and surface geology as inferred from the Fig. 4.11



LEGEND

x. Accepted depth point.

Quaternary — Chad Formation

Tertiary — Basalts; Kerri Kerri Formation

F — — F' Fault approximation

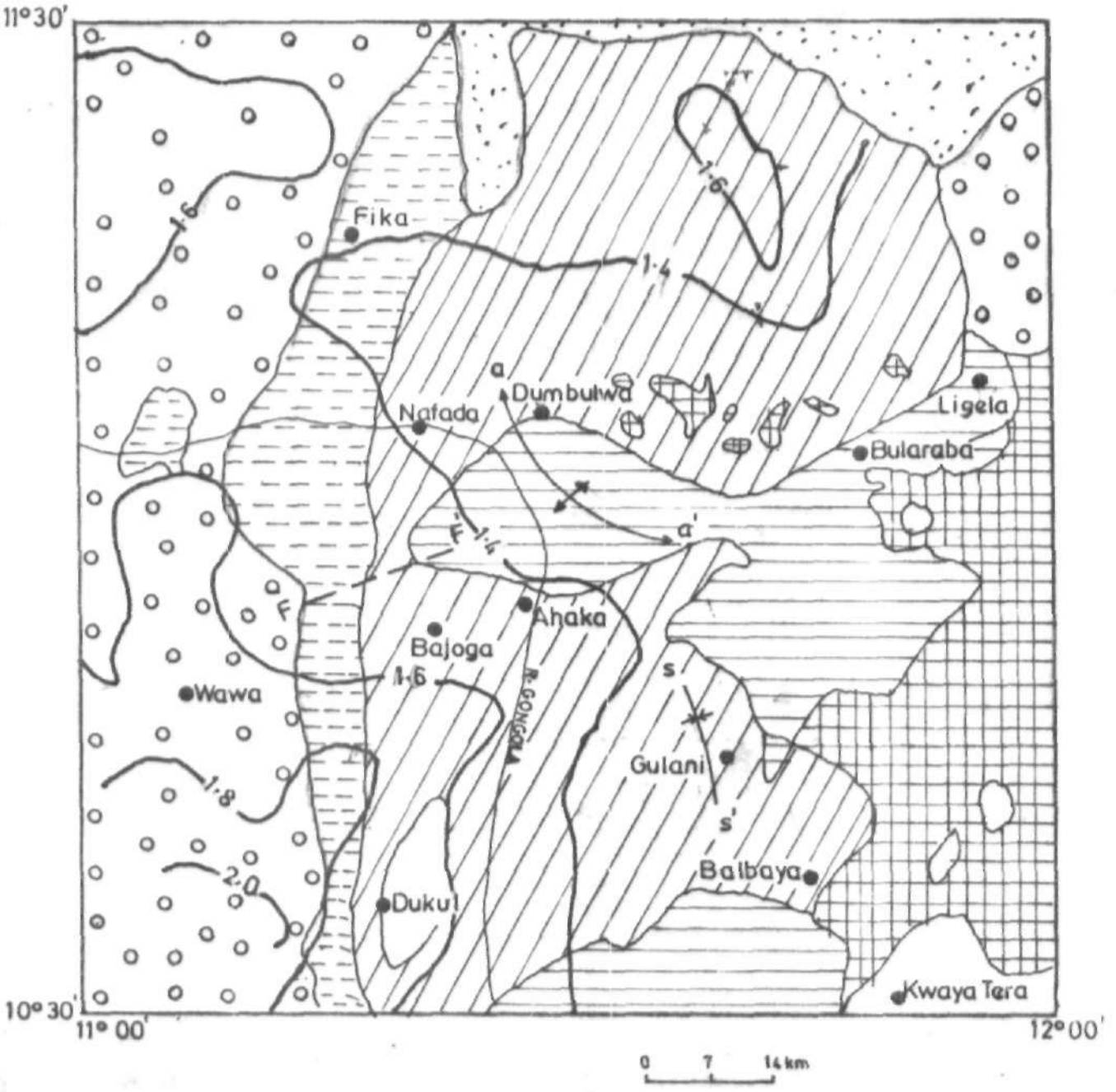
Antictinal axis

Synclinal axis

Cretaceous — Gombe Sandstone; Pindiga Formation; Bima Sandstone

Precambrian & Uppercambrian — Basement Complex

Fig. 4: 10 Geological Map of study area showing the positions of depths used in preparing the magnetic basement map of the area.



314056

LEGEND

Quarternary — Chad Formation

Tertiary — Basalts; Kerri Kerri Formation

Cretaceous — Gombe Sandstone; Pindiga Formation; Bima Sandstone

F---F' Fault approximation

Antictinal axis

Synclinal axis

Precambrian & Uppercambrian — Basement Complex

Fig. 4.11. Combined magnetic basement map and surface geology of area.

indicates that the basement dips away from under the Biu Plateau toward the Kerri-Kerri formation in the west and Chad formation in the north. The steepest section of the basement is located in the Kerri-Kerri formation west of Dukul. In this region, the depths reach between 1.8 Km and 2.0 Km which is close to the depth of 1.97 Km obtained further south of Ako, from gravity interpretation (Okafo, 1982).

There is, however, no apparent relationship between the basement structure and the major lineament which appear to cross the region. This may be due in part to insufficient resolution of the basement map or to the fact that the lineaments are not caused by structures but by variation in magnetization of the rocks. This heterogeneous magnetic character of the basement in the Benue trough has been noted in other studies (Ofoegbu, 1985).

DISCUSSION AND CONCLUSION

5.1 Summary and Discussion of Results.

Werner convolution method has been used with moderate success in basement study of a section of the Benue Trough within latitude $10^{\circ}30'N$ to $11^{\circ}30'N$ and longitude $011^{\circ}00'E$ to $012^{\circ}00'E$. The aeromagnetic data used was derived from maps provided by Geological Survey of Nigeria. The data was sampled at an interval of 0.5 Km (later reduced to 0.25 Km by linear interpolation) along profiles with a spacing of approximately 2 Km. The data coverage made it possible to correlate results from adjacent profiles. The basement surfaces were estimated by correlating results from adjacent profiles. Calculated depth from the interpreted surfaces were selected for compilation of a basement map of the study area.

In general depth to the basement varies between 1.4 Km and 2.0 Km. A comparison with the results of previous estimates from gravity and magnetic data indicates that the basement depths obtained in the present work conform well with other geophysical estimates. For example, on the basis of gravity and magnetic anomalies over the Upper Benue region, Osazuwa (1978) and Osazuwa et al., 1981 obtained sedimentary thickness ranging from 0.9 Km to 2.2 Km for gravity data and 0.9 Km to 4.9 Km from magnetics. Also Nwogbo (1987) carried out a detailed interpretation of aeromagnetic

data from the whole of the Upper Benue using spectral analysis and obtained basement depths betwee 2.0 Km to 2.83 Km. In the present areas of study, the deepest part of the basement is 2 Km deep located south of Wawa under the Kerri-Kerri formation. This depth is similar to that obtained by Okafor (1982) in an interpretation of a gravity profile between Bauchi and Gombe in which a maximum depth of 1.97Km was obtained at Ako south of Wawa.

One important observation from comparing the magnetic intensity profiles and the interpreted basement surface(Fig. 4.5 to Fig. 4.8)is that the basement topography cannot totally account for all the magnetic intensity variation in the area. Reasons for this were earlier suggested to include poor resolution of the basement maps and the heterogeneous magnetic character of the basement rocks. This latter characteristics of the basement rocks in the Benue Trough has been noted in other studies (Ofoegbu, 1985), and it was suggested that the observed magnetic intensity variation over the area could best be explained by a combination of variable basement topography, and the presence of intrusive bodies. Although no attempt was made to model the intrusive bodies in this study because such a task goes slightly beyond the scope of our initial objectives, an inspection of the profiles indicated that the suggestion of intrusives is a reasonable one. The apparent lack of corresponding basement structures

to support the presence of magnetic lineaments suggested by other workers may therefore be due to the fact that the lineaments are not caused by basement structures but by changes in magnetization.

5.2 Conclusion

This study has shown that the Werner deconvolution technique can be a quick and reliable method of interpreting the magnetic anomalies. However, the reliability of the results depend on the quality of the data used. From this point of view, data digitised from contoured maps are not the most ideal for determination of shallow structures. In this study it was found that the basement below the sedimentary formations lies between a depth of 1.4 Km and 2.0 Km with the deepest parts located between Wawa and Dukul. Qualitative interpretation shows the presence of some lineaments up to about 100 Km across the study area. These could not be related to basement structures and appears to be caused by variation in magnetization.

Finally since the results obtained when using the Werner deconvolution method depends to a large extent on the quality of the data and digitizing interval, it is suggested that point data should be used for future studies especially in shallow basement areas.

REFERENCES

Adighije, C. (1979). Gravity field of Benue Trough, Nigeria. Nature Phys. Sci., pp 199-210.

Adighije, C. (1981a). Gravity Study of Lower Benue Trough, Nigeria. Geol. Mag.. 118, pp.50-67

Adighije, C. (1981b). A gravity Interpretation of the Benue Trough, Nigeria Tectonophysics 79, pp. 109 - 128.

Ajakaiye, D.E. (1981). Geophysical Investigations in the Benue Trough - a review. Earth Evolution Sci., 2, pp 11-125.

Ajakaiye, D.E. and Burke, K., (1973). A Bouger gravity Map of Nigeria. Tectonophysics 16, pp. 103-115.

Ajakaiye, D.E.; Hall, D.H. and Millar, T.W. (1985). Interpretation of aeromagnetic data across the central crystalline shield area of Nigeria. Geophys. J.R. astr. Soc., 83, pp. 503-517.

Ajakaiye, D.E.; Hall, D.H. Millar, T.W.; Verheijen, P.J.T.; Awad, M.B.; and Ojo S.B. (1986). Aeromagnetic anomaly and tectonic trends in and around the Benue Trough, Nigeria. Nature Phys. Sci., 319 (6054), pp.582-584.

Ajayi, C.O. and Ajakaiye, D.E. (1981). The Origin and peculiarities of the Nigerian Benue Trough: another look from recent gravity data obtained from the Middle Benue. Tectonophysic, 80, pp. 285-303.

Artsybashev, V.A. and Kogbe, C.A. (1975). Crustal Structure of the Benue Valley area Nigeria. Geol. Rdsch. 64, pp. 324-329.

Avbovbo, A.A. (1980), Basement geology in sedimentary basis of Nigeria. Geology, V. 8, pp. 323-327.

Carter, J.D.; Barber, W. and Tait, E.A.(1963). The geology of parts of Adamawa, Bauchi and Borno provinces in NorthernNigeria. Bull. geol. surv. Nigeria, No. 30.

Cratchley, C.B. and Jones, G.P. (1965). An interpretation of the geology and gravity anomalies of the Benue Valley, Nigeria. Geophys. Pap. Overseas geol. Surv. London No; 1.

Dobrin, M.B., (1976), Geophysical Prospecting, 2nd ed: New York, McGraw-Hall Publishers inc.

Domzalski, W. (1966). Importance of Aeromagnetic in Evaluation of Structural Control of Mineralization. Geophysical Prospecting, 14, pp. 273-291.

Friedberg, J.C., (1975). Understanding and use of Werner Deconovolution in Aeromagnetic Interpretation. Aero Services Corporation, Houston, Textas, pp. 1 - 29.

Gay, S.P. (Jr) (1963). Standard Curves for Interpretation of magnetic anomalies over long tabular bodies. Geophysics, 28, pp. 161-200.

Grant, F.S. and West. G.F., (1965). Interpretation Theory in Applied Geophysics. McGraw-Hill Book company, New York.

Griffiths, D.H. and R.F. King (1965). Applied Geophysics for Engineers and Geologists. Pergamon Press.

Hartman, R.R. Teskey, D.J., and Friedberg J.L. (1971). A system for rapid digital aeromagnetic interpretation. Geophysics V. 36, pp. 891-918.

Hjett, S.E. (1973) Experience with automatic magnetic interpretation using the thick plate model: Geophysical prospecting V. 21, pp. 243-265.

Hutchison, R.D. (1958). Magnetic Anomalies by Logrithimic Curves. Geophysics, 23, pp. 749-769.

Jain, S., (1976). An authomatic method of direct interpretation of magnetic profiles. Geophysics. V. 41, pp.531-541.

Ku, G.C. and Sharp, J.A. (1983). Werner deconvolution for automated magnetic interpretation and its refinement using Marquardts inverse modelling. Geophysics, V. 48, No.6, pp. 754-774.

Kevin, T.K., (1983) Werner deconvolution of profiles potentials field data. Geophysics V. 48, pp. 234-237.

Kilty, K.T.(1983) Werner deconvolution of profiles potential field data. Geophysics, V. 48, No.2, pp.234-237.

Mittal, P.K. (1984). Alogrithm for error adjustment of potential field data along a survey network (short note). Geophysics, V. 49, No. 4, pp 467-469.

Myada, E.E. (1979). Mafa-Dikwa geophysical anomalies and their interpretation. Unpublished Ph.D. thesis. Ahmadu Bello University, Zaria, Nigeria.

Naidu, P.S. (1969). Estimation of spectrum and cross spectrum of aeromagnetic fields using fast digital Fourier transform (FDFT) techniques. Geophysical

Nettleton, L.L. (1971). Elementary Gravity and Magnetics For Geologists and Sesmologists (Monograph series). Society of Exploration Geophysicists. Tulsa, United States of America.

Nwogbo, P.O. (1987). Spectral analysis and interpretation of aeromagnetic anomalies over the Upper Benue Trough. Nigeria. Unpublished M.Sc. Thesis, Ahmadu Bello University, Zaria, Nigeria.

Offodile, M.E. (1976). A review of the Geology of the Cretaceous of the Benue Valley. In: Kogbe C.A. (Ed.) Geology of Nigeria - Elizabeth Pub. Co. Lagos pp. 319.330.

Offodile, M.E. (1977). The economic significance of some of the Cretaceous events in the Benue Valley. J.Min. and Geol., 14(2): pp67 (abstract).

Ofoegbu, C.O. (1984a). Interpretation of aeromagnetic anomalies over the Lower and Middle Benue Trough of Nigeria. Geophys. J.R. astr. Soc., 79, pp. 813-823.

Ofoegbu, C.O. (1984b) An aeromagnetic study of the Lower Benue Trough, Nigeria. Revista Brasileira de Geociencias, 14(1). pp. 54 -59.

Ofoegbu, C.O. (1985). Interpretation of an aeromagnetic profile across the Benue Trough J. Afric. Earth Sci., 3(3): pp. 293 - 297.

Okafo, B.J.O. 1982 Notes on the gravity profiles Between Bauchi and Gombe across the Kerri-Kerri formation. Paper presented at the 8th Annual Conference of the Nigerian Mining and Geoscienceses society; Kaduna. 28th February - 5th March, 1982.

Osazuwa, I.B. (1978). Gravity and Magnetic Survey of the Upper Benue Trough. Unpublished M.Sc. thesis. Ahmadu Bello University, Zaria Nigeria.

Osazuwa, I.B.; Ajakaiye, D.E. and Verheijen, P.J.T. (1981). Analysis of the Structure of part of the Upper Benue rift Valley on the Basis of New geophysical data. Earth Evolution Sci., 2,pp

Peters, L.J., (1949), The Direct approach to magnetic Interpretation and its practical applications: Geophysics. V. 14, pp. 200-320.

Talwani, M. and Ewing, M., 1960. Rapid computation of gravitational attraction of three-dimensional bodies of arbitrary shape. Geophysics, V., 25, pp. 126-135.

Talwani, M. and Heirtzler, J. (1964). Computation of magnetic anomalies caused by two-dimensional structures of arbitrary shape. In: Parks, G.A. (Ed.). Computers in Mineral Industries.

Telford, W.M., Geldart, L.P., Sheriff, R.E., and Keys, D.A., (1976). Applied Geophysics, Cambridge University Press.

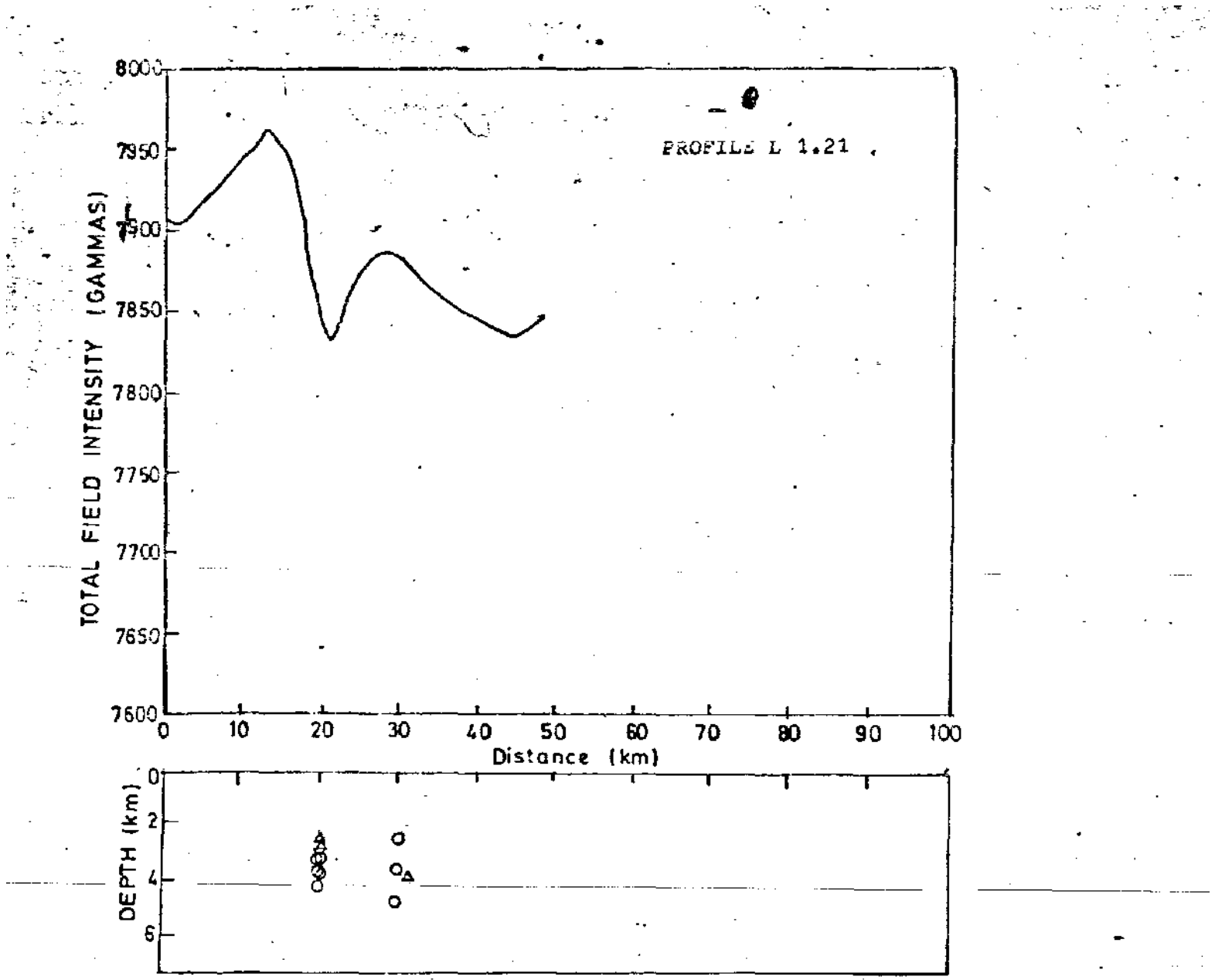
Vacquier, V., Steenland, N.C., Henderson. R.O., and Zietz I., (1951). Interpretation of Aeromagnetic Maps, Geol. Soc., Am., Mem. 47.

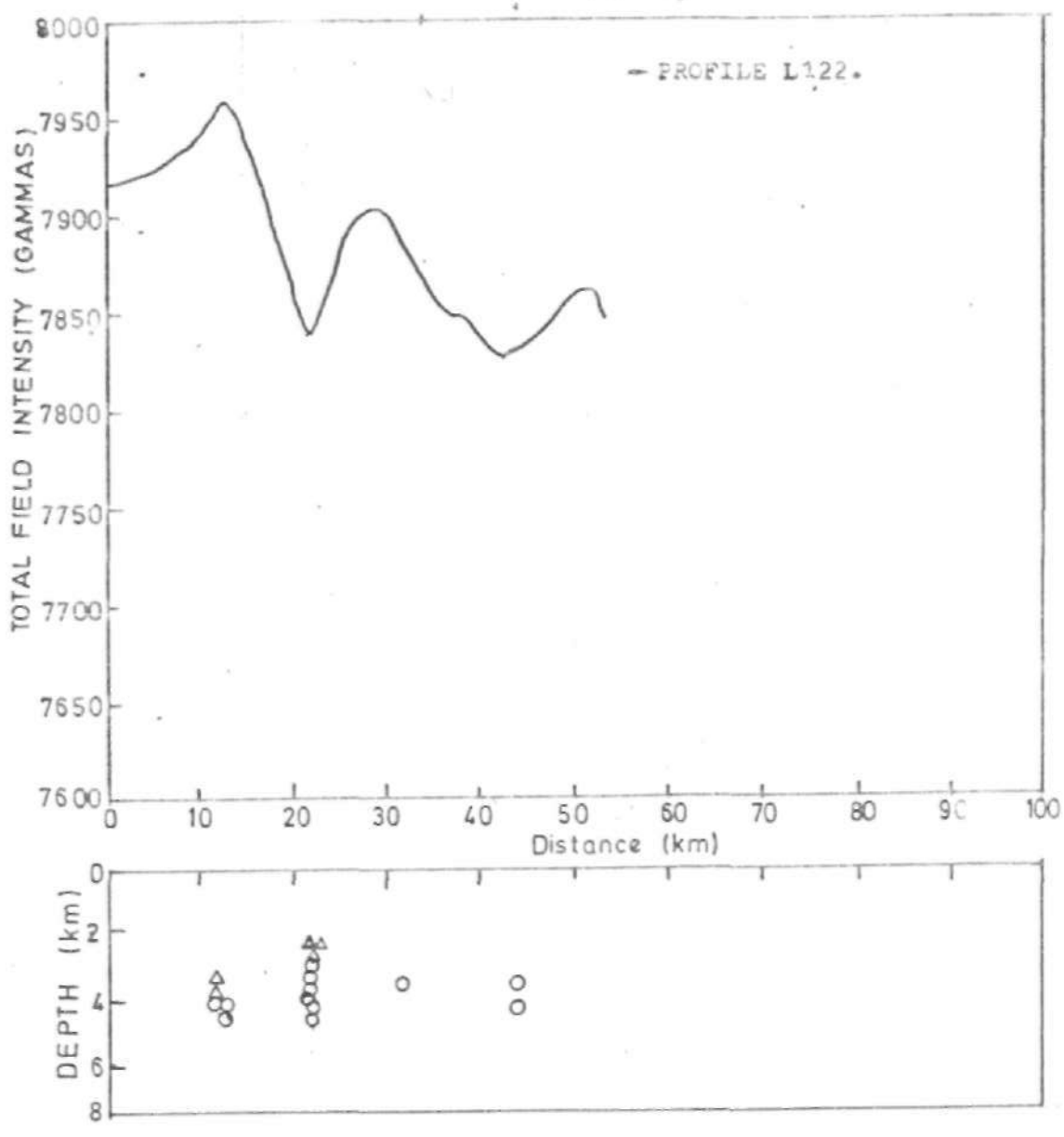
Wright, J.B. (1976). Origins of the Benue Trough: a critical review. In: Kogbe, C.a. (Ed.). Geology of Nigeria - Elizabeth Pub. Co., Lagos.

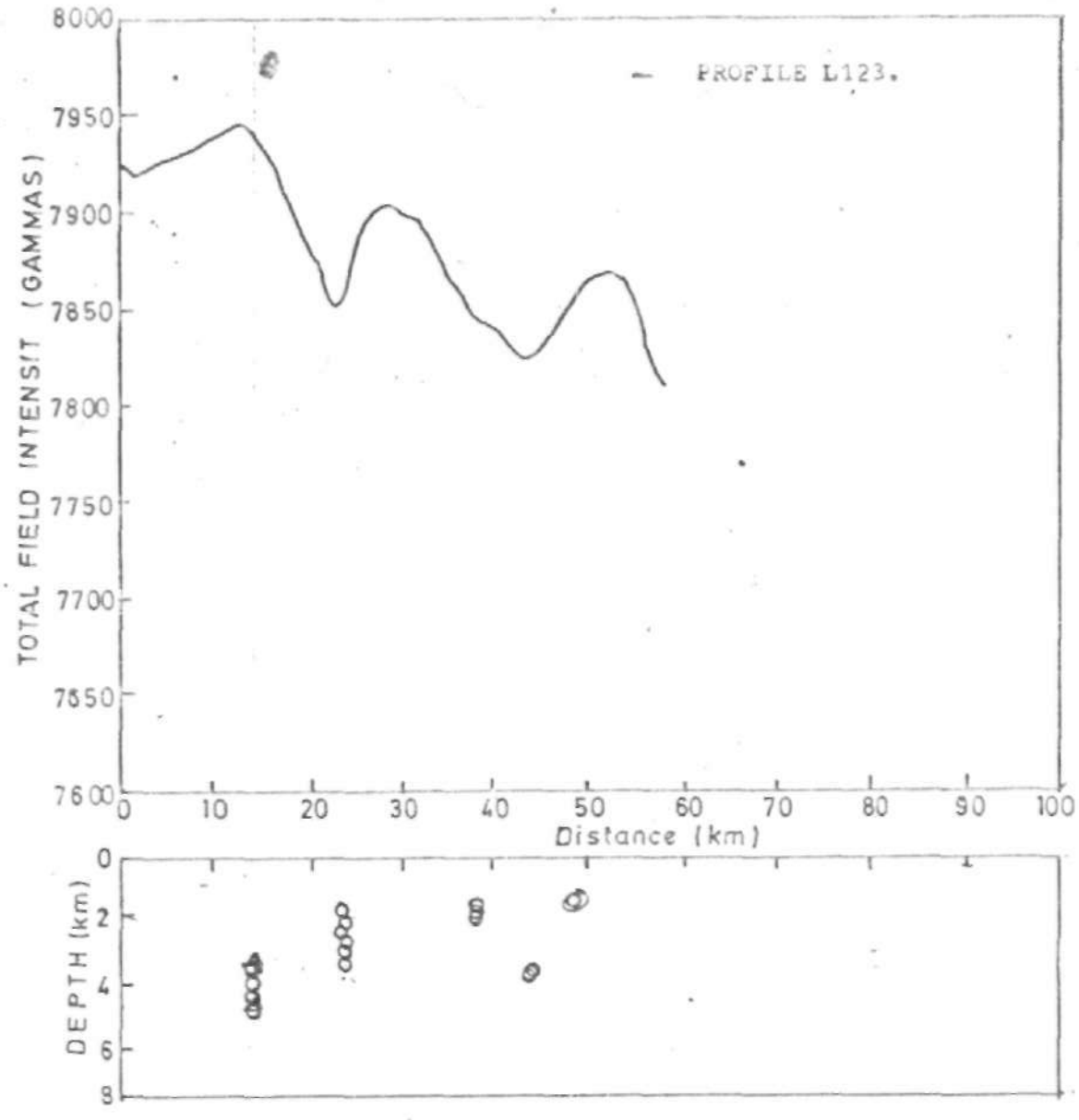
Werner, S. (1953) Interpretation of magnetic anomalies at sheet-like bodies: Sveriges Geologisks undersokning, Ser. e.. No 508.

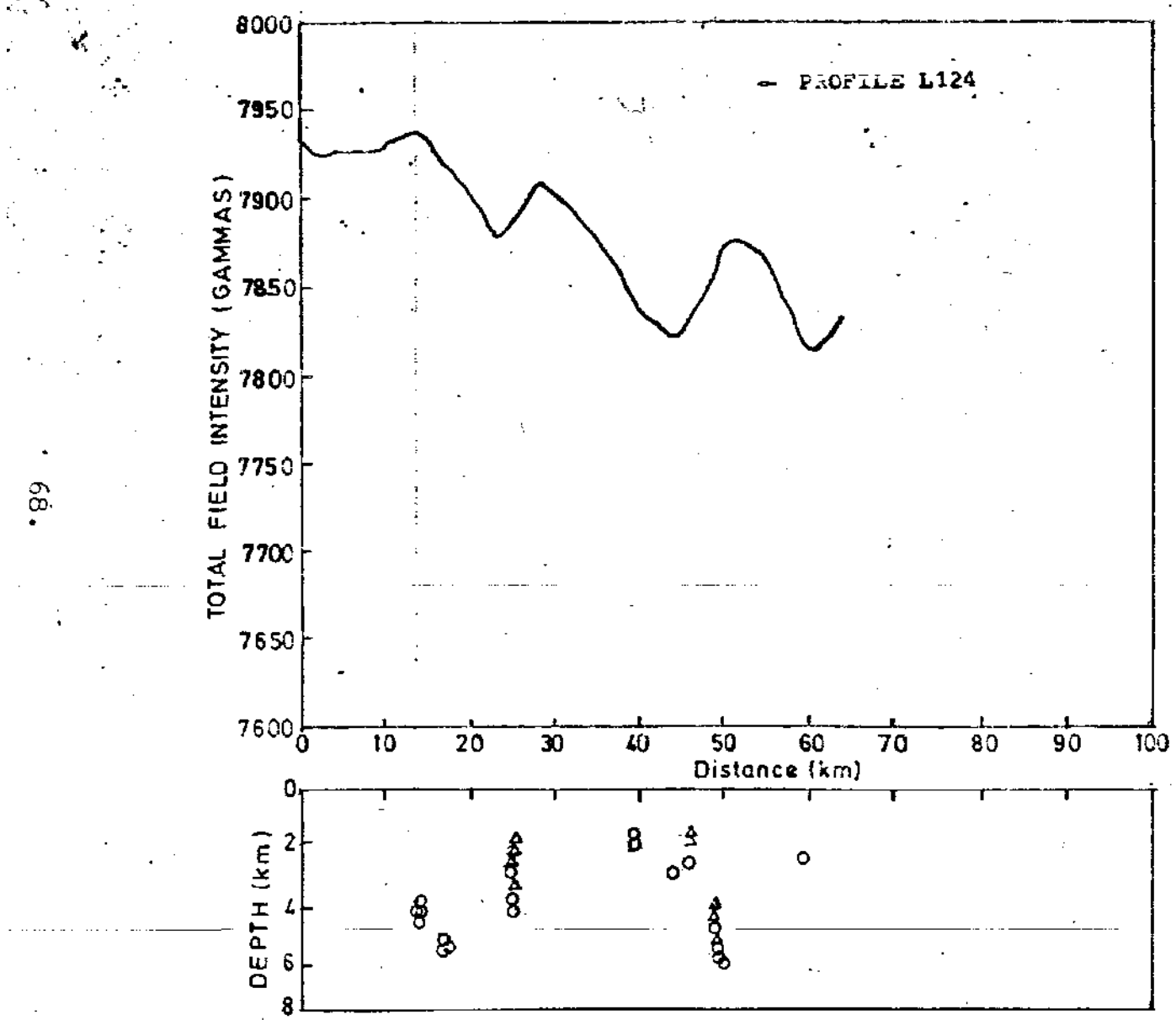
A P P E N D I X

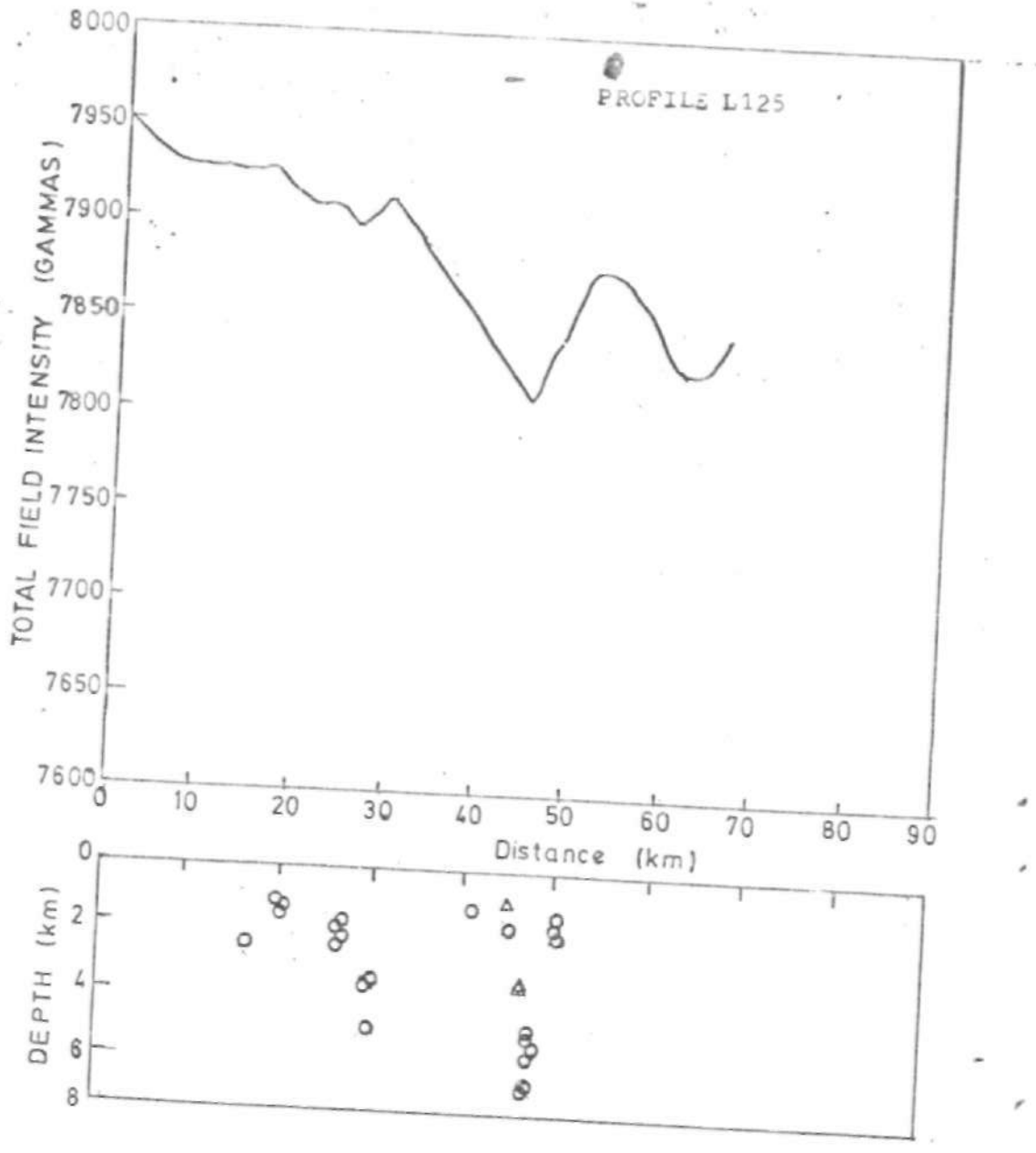
Plots showing Werner deconvolution of some selected field profiles. The symbols o and Δ represent calculted depths for total magnetic field and the derivative respectively.

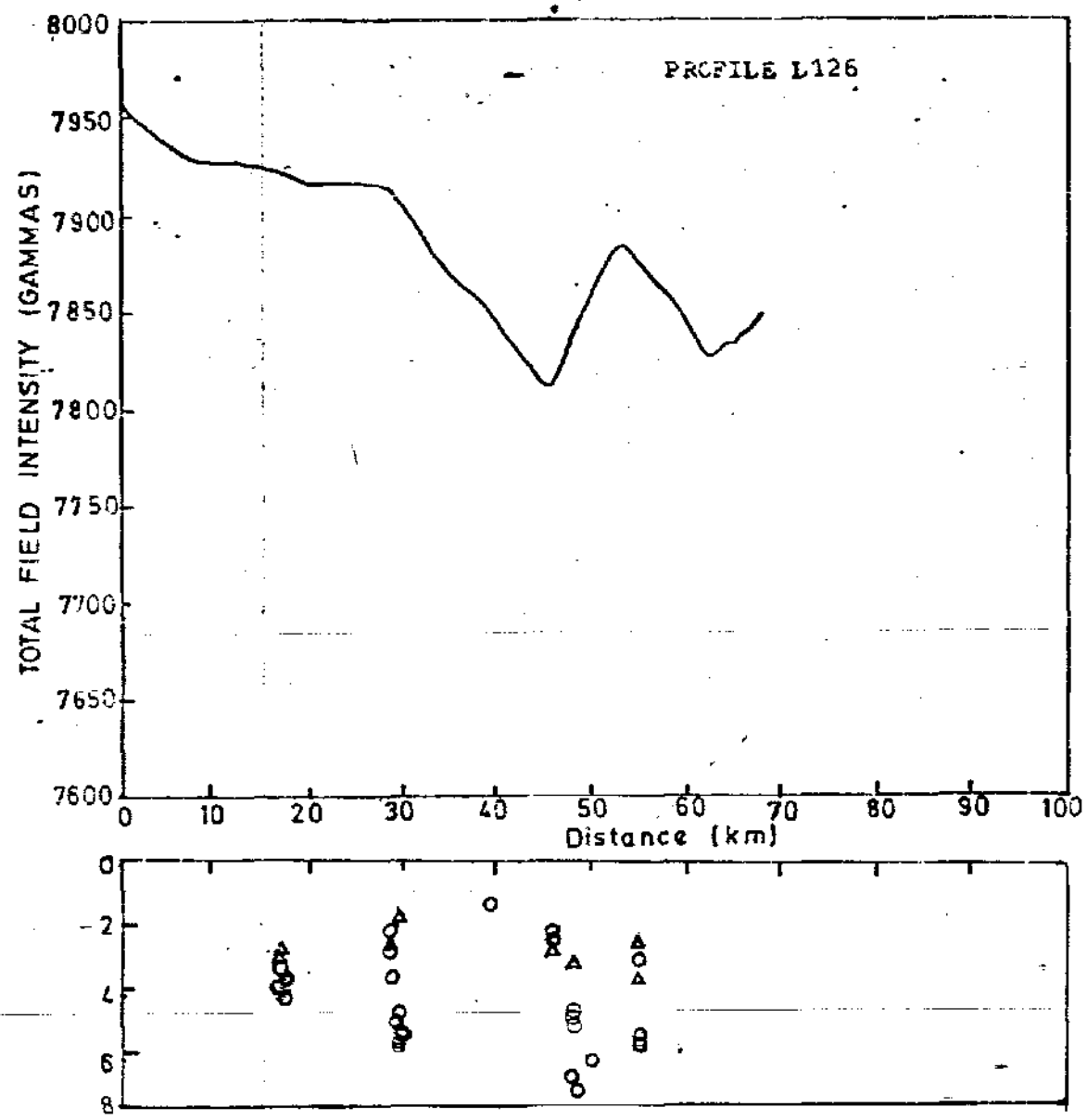

PROFILE L 1.21
TOTAL FIELD INTENSITY (GAMMAS)
8000
7950
7900
7850
7800
7750
7700
7650
7600
0
10
20
30
40
50
60
70
80
90
100
Distance (km)
DEPTH (km)
0
2
4
6

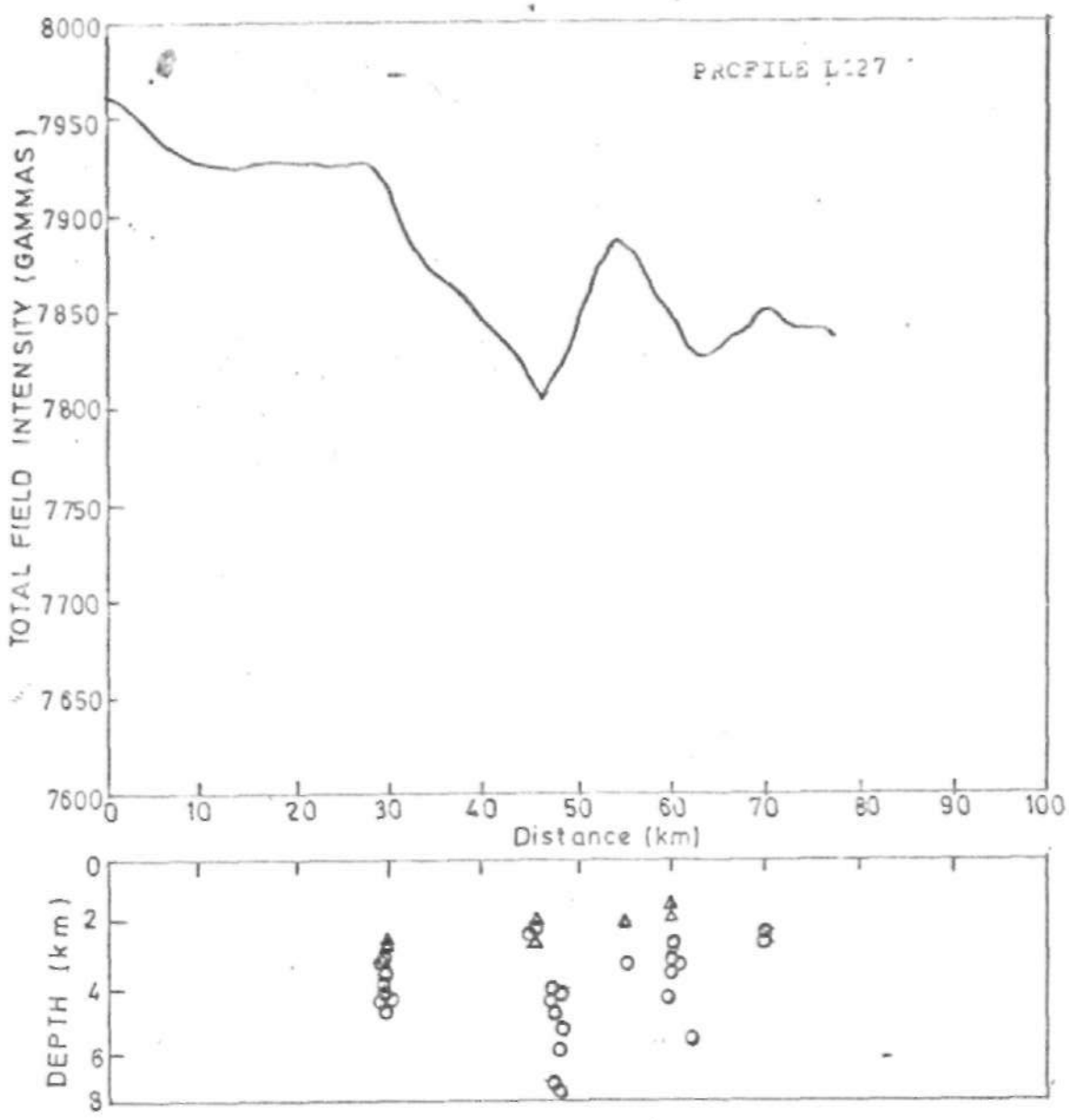

— PROFILE L122.
TOTAL FIELD INTENSITY (GAMMAS)
8000
7950
7900
7850
7800
7750
7700
7650
7600
0
10
20
30
40
50
60
70
80
90
100
Distance (km)
DEPTH (km)
0
2
4
6
8

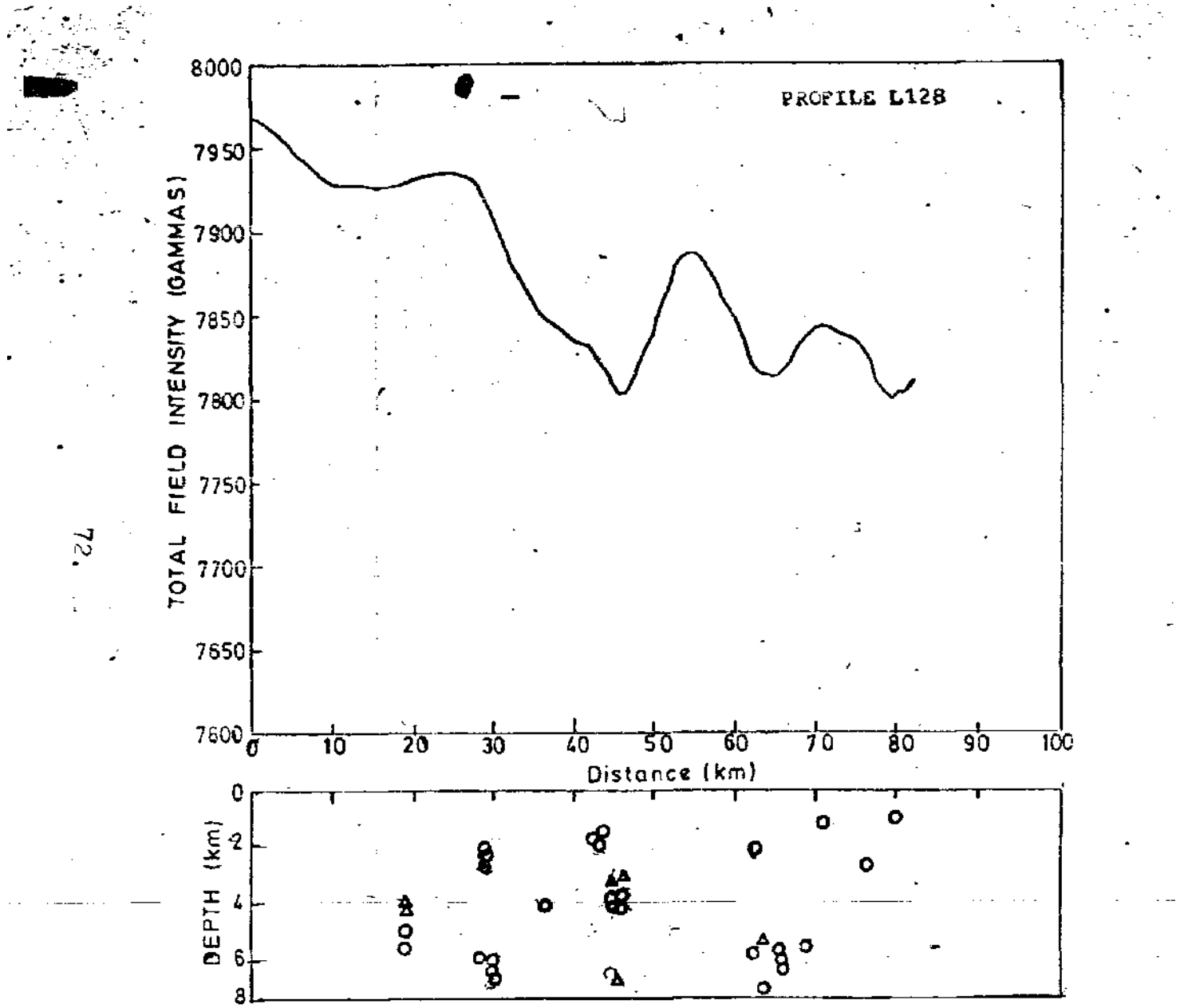

PROFILE L123.
TOTAL FIELD INTENSIT (GAMMAS)
8000
7950
7900
7850
7800
7750
7700
7650
7600
0
10
20
30
40
50
60
70
80
90
100
Distance (km)
DEPTH (km)
0
2
4
6
8

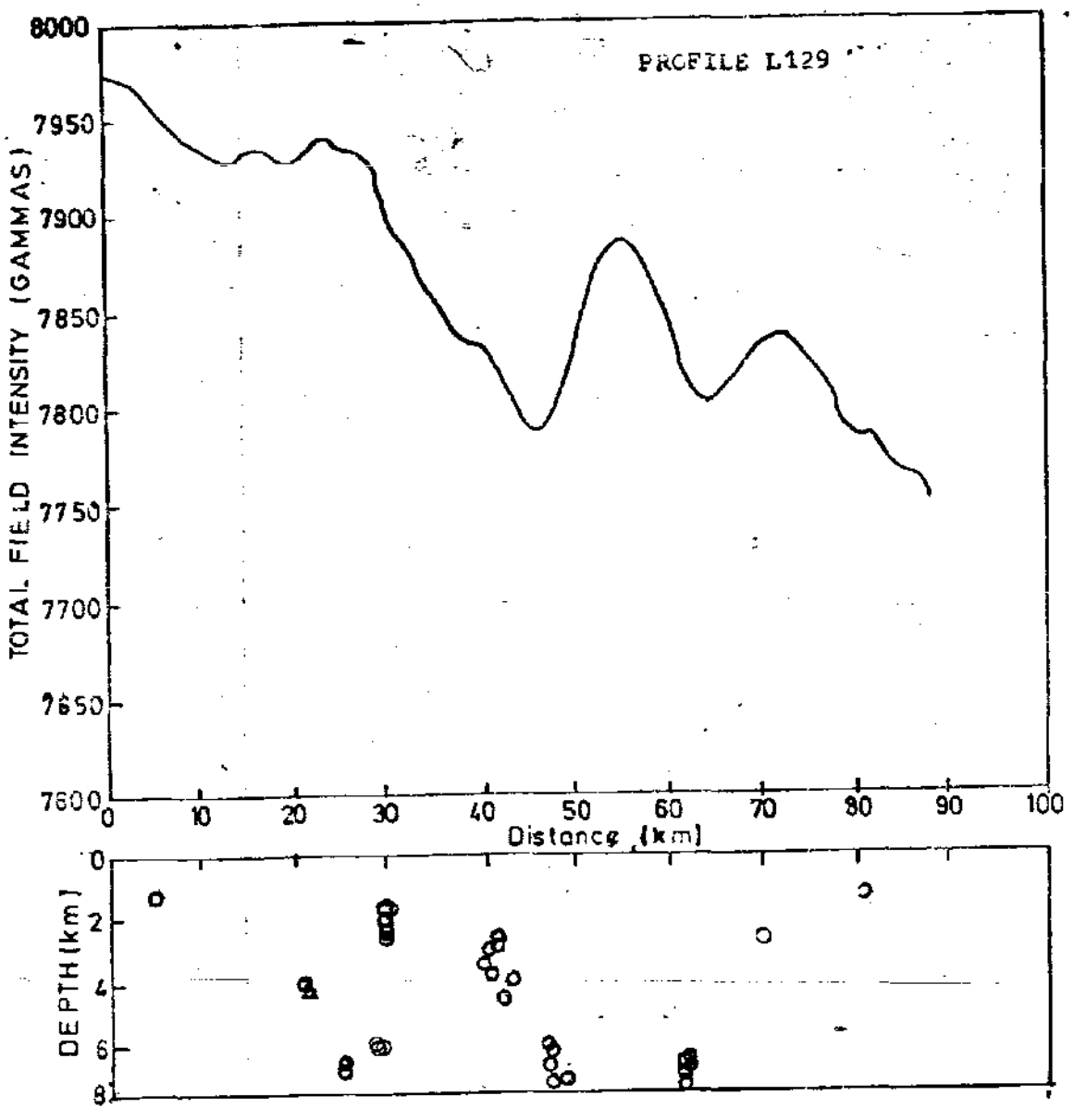

PROFILE L124
TOTAL FIELD INTENSITY (GAMMAS)
8000
7950
7900
7850
7800
7750
7700
7650
7600
0
10
20
30
40
50
60
70
80
90
100
Distance (km)
DEPTH (km)
0
2
4
6
8

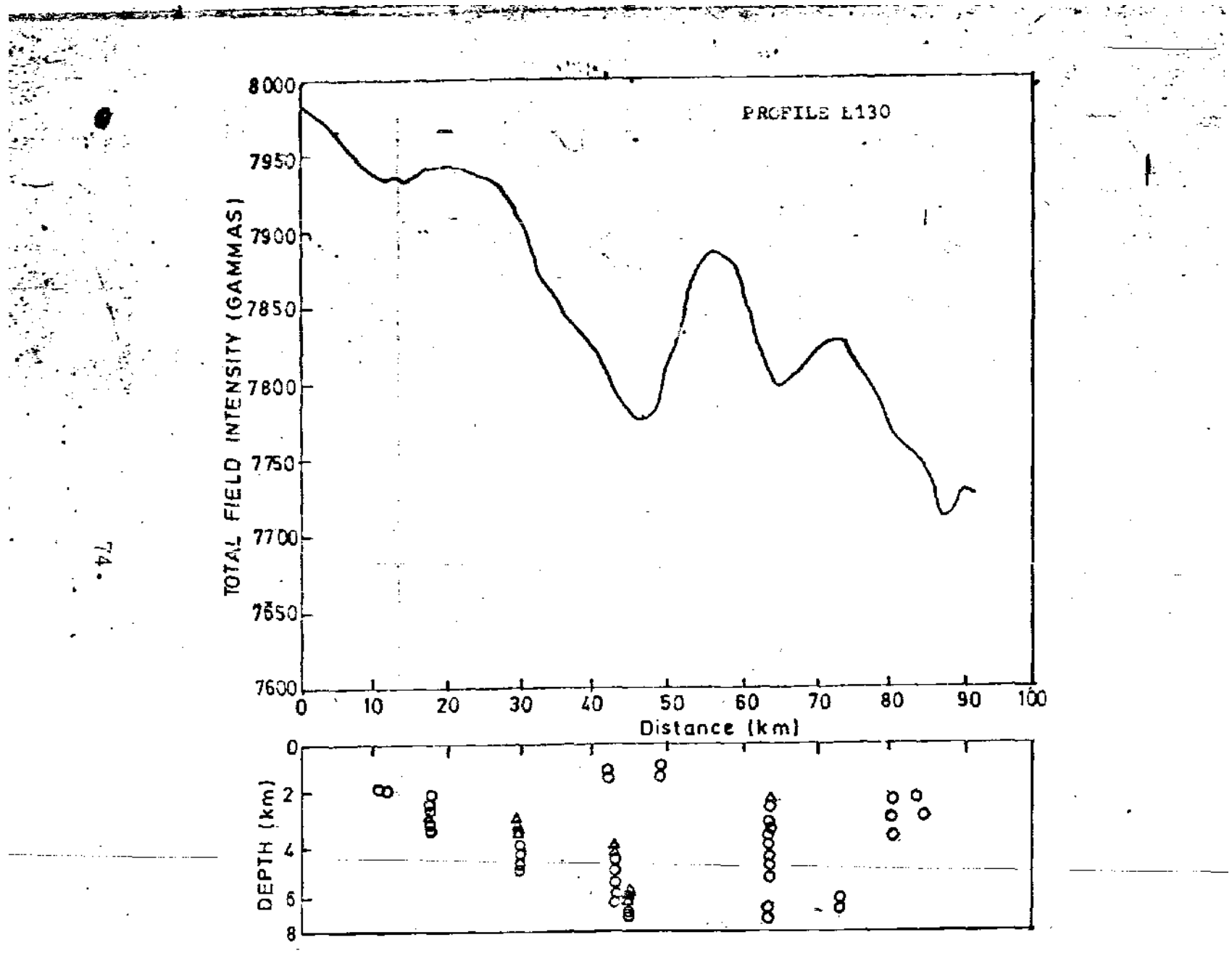

PROFILE L125
TOTAL FIELD INTENSITY (GAMMAS)
8000
7950
7900
7850
7800
7750
7700
7650
7600
0
10
20
30
40
50
60
70
80
90
Distance (km)
DEPTH (km)
0
2
4
6
8

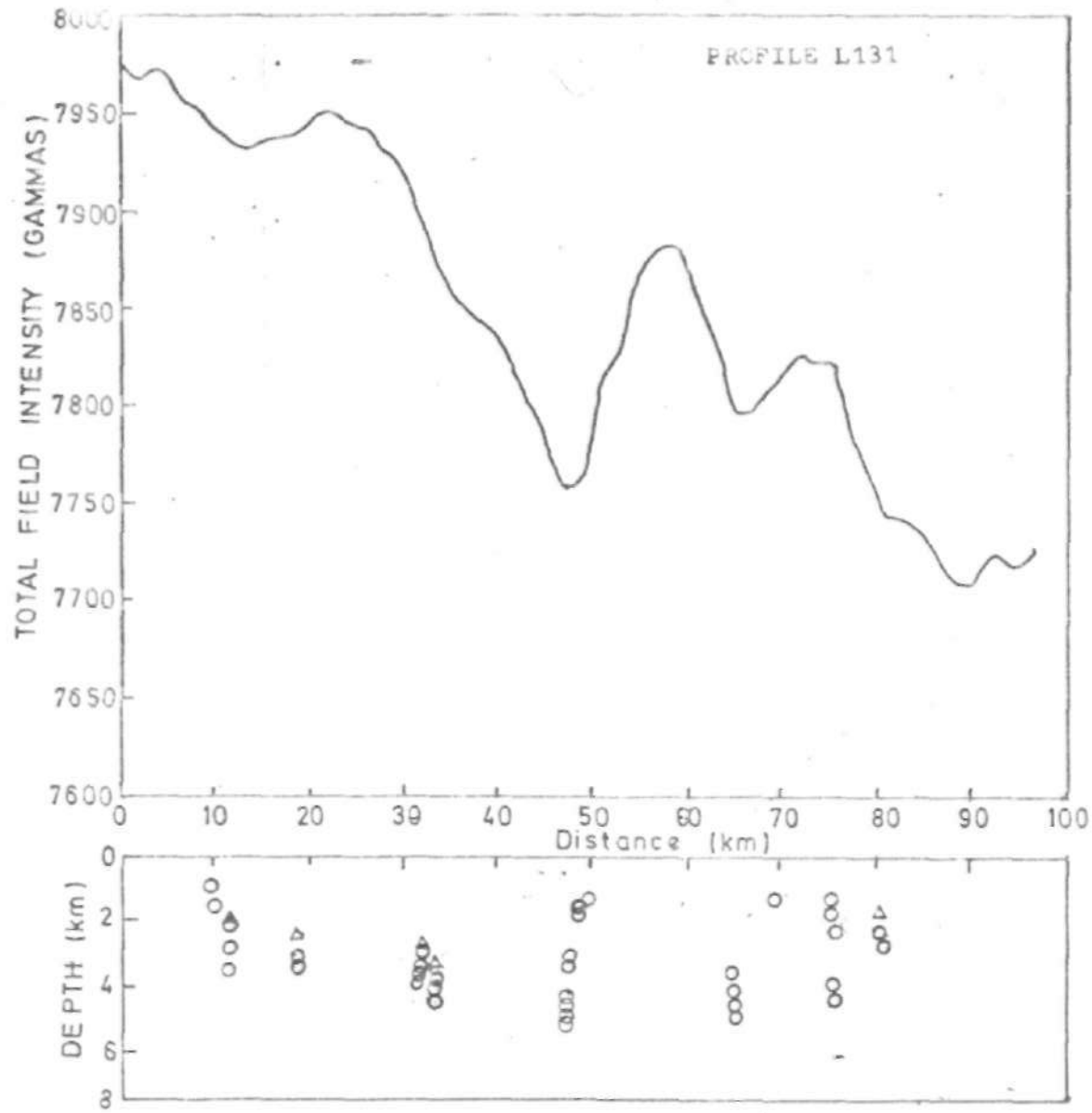

PROFILE L126
TOTAL FIELD INTENSITY (GAMMAS)
8000
7950
7900
7850
7800
7750
7700
7650
7600
0
10
20
30
40
50
60
70
80
90
100
Distance (km)
0
2
4
6
8

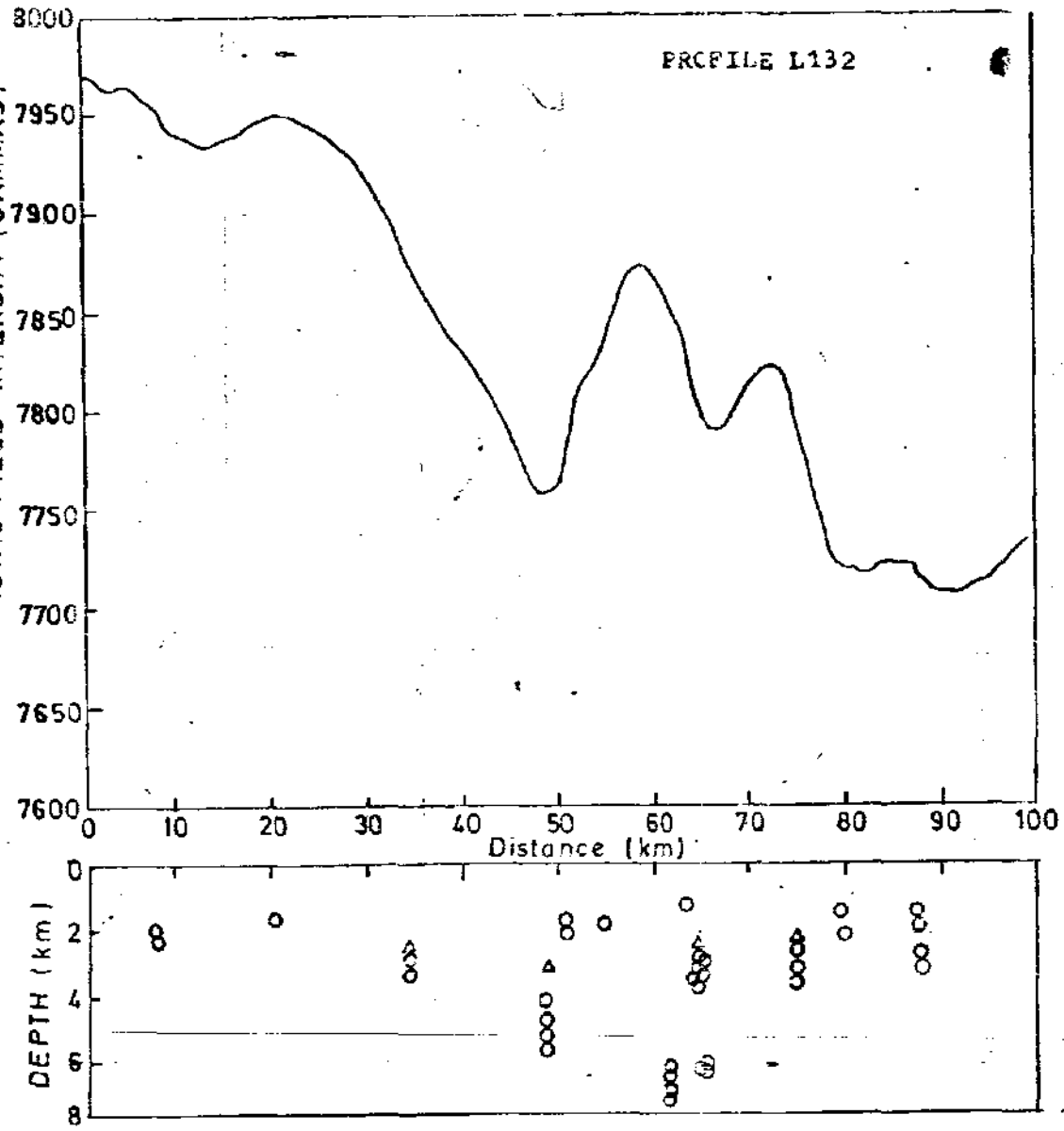

PROFILE L-27
TOTAL FIELD INTENSITY (GAMMAS)
8000
7950
7900
7850
7800
7750
7700
7650
7600
0
10
20
30
40
50
60
70
80
90
100
Distance (km)
DEPTH (km)
0
2
4
6
8

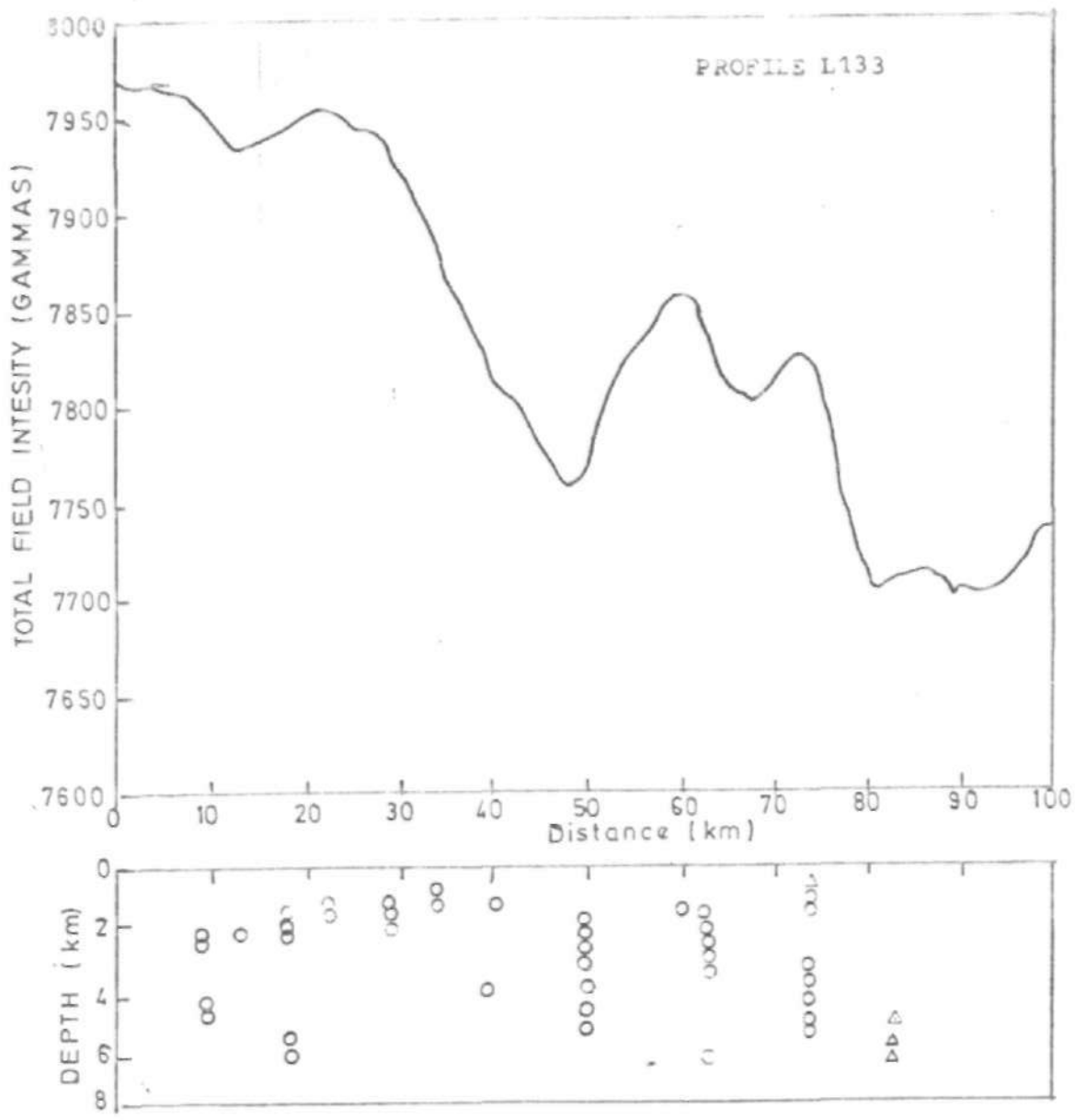

PROFILE L128
TOTAL FIELD INTENSITY (GAMMAS)
8000
7950
7900
7850
7800
7750
7700
7650
7600
0
10
20
30
40
50
60
70
80
90
100
Distance (km)
DEPTH (km)
0
2
4
6
8

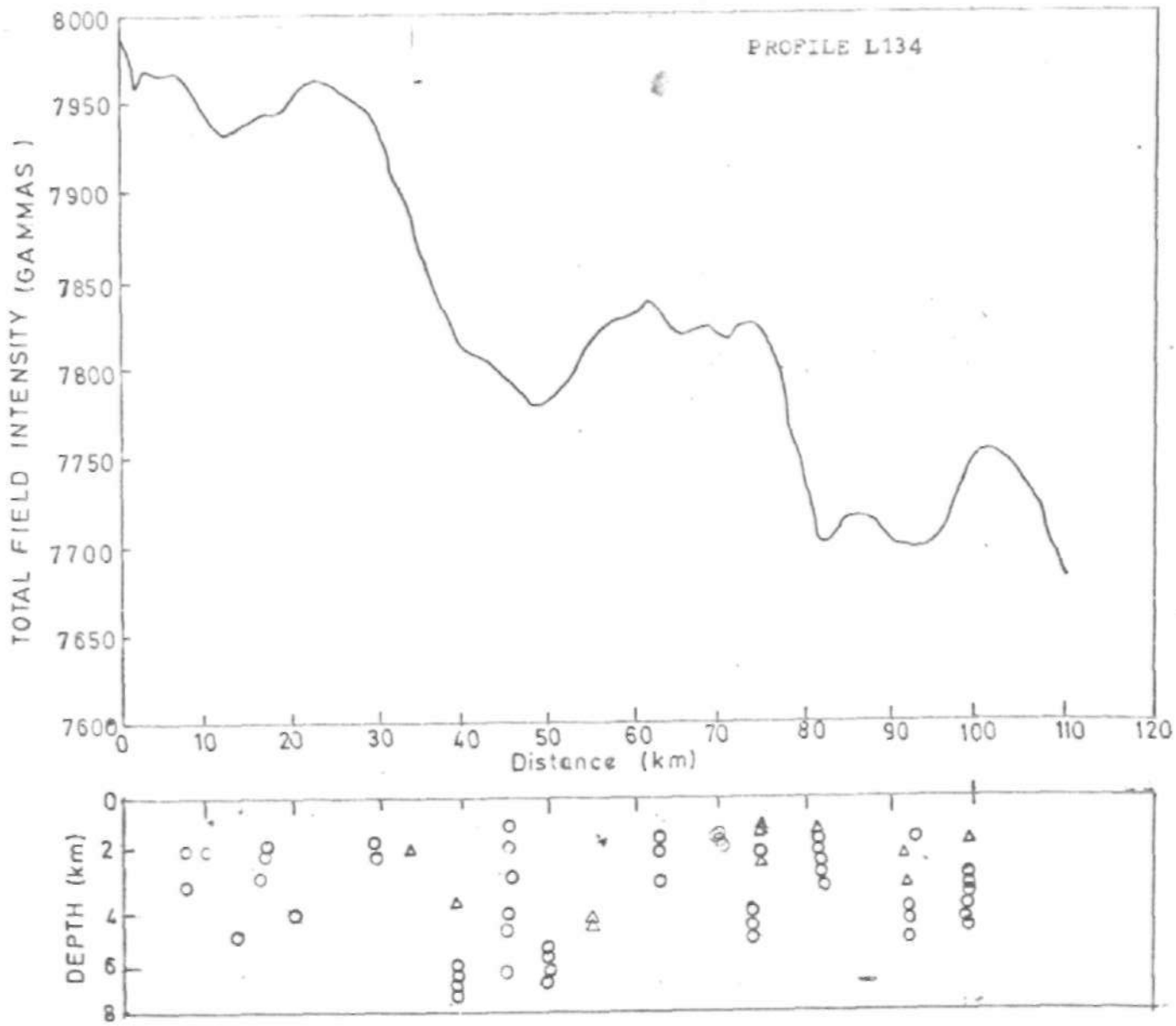

PROFILE L129
TOTAL FIELD INTENSITY (GAMMAS)
8000
7950
7900
7850
7800
7750
7700
7650
7600
0
10
20
30
40
50
60
70
80
90
100
Distance (km)
DEPTH (km)
0
2
4
6
8

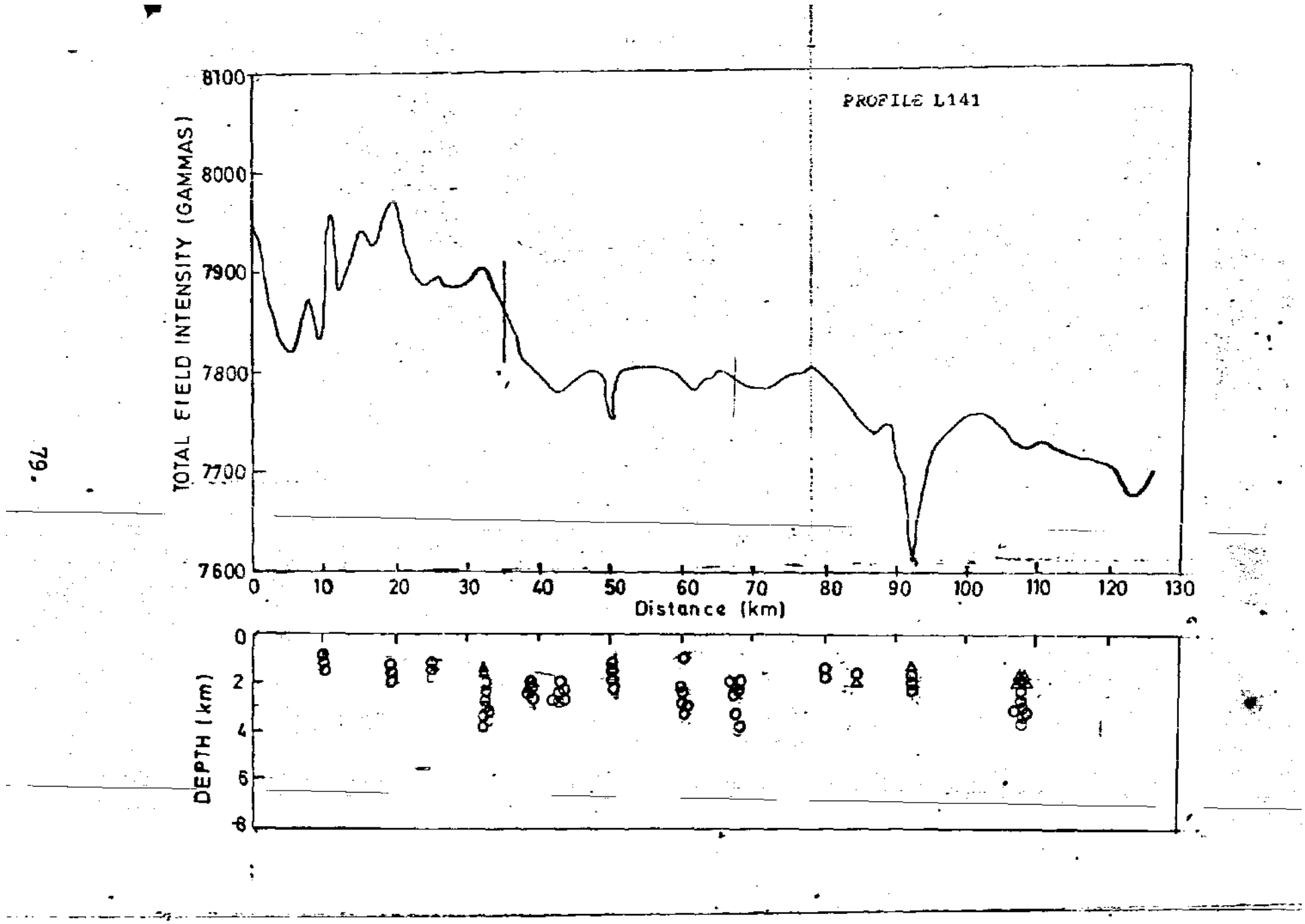

PROFILE L130
TOTAL FIELD INTENSITY (GAMMAS)
8000
7950
7900
7850
7800
7750
7700
7650
7600
0
10
20
30
40
50
60
70
80
90
100
Distance (km)
DEPTH (km)
0
2
4
6
8

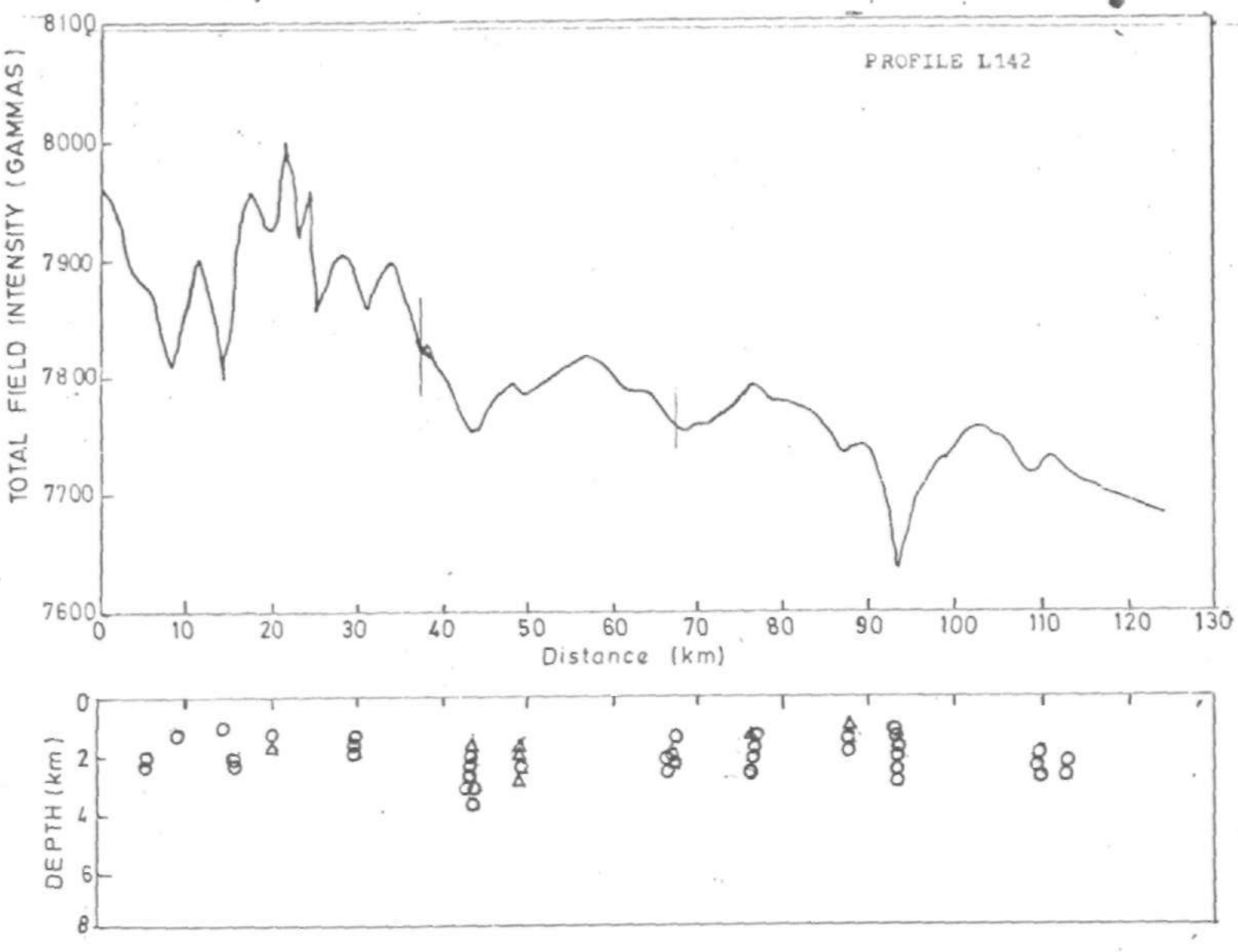

PROFILE L131
TOTAL FIELD INTENSITY (GAMMAS)
8000
7950
7900
7850
7800
7750
7700
7650
7600
0
10
20
30
40
50
60
70
80
90
100
Distance (km)
DEPTH (km)
0
2
4
6
8

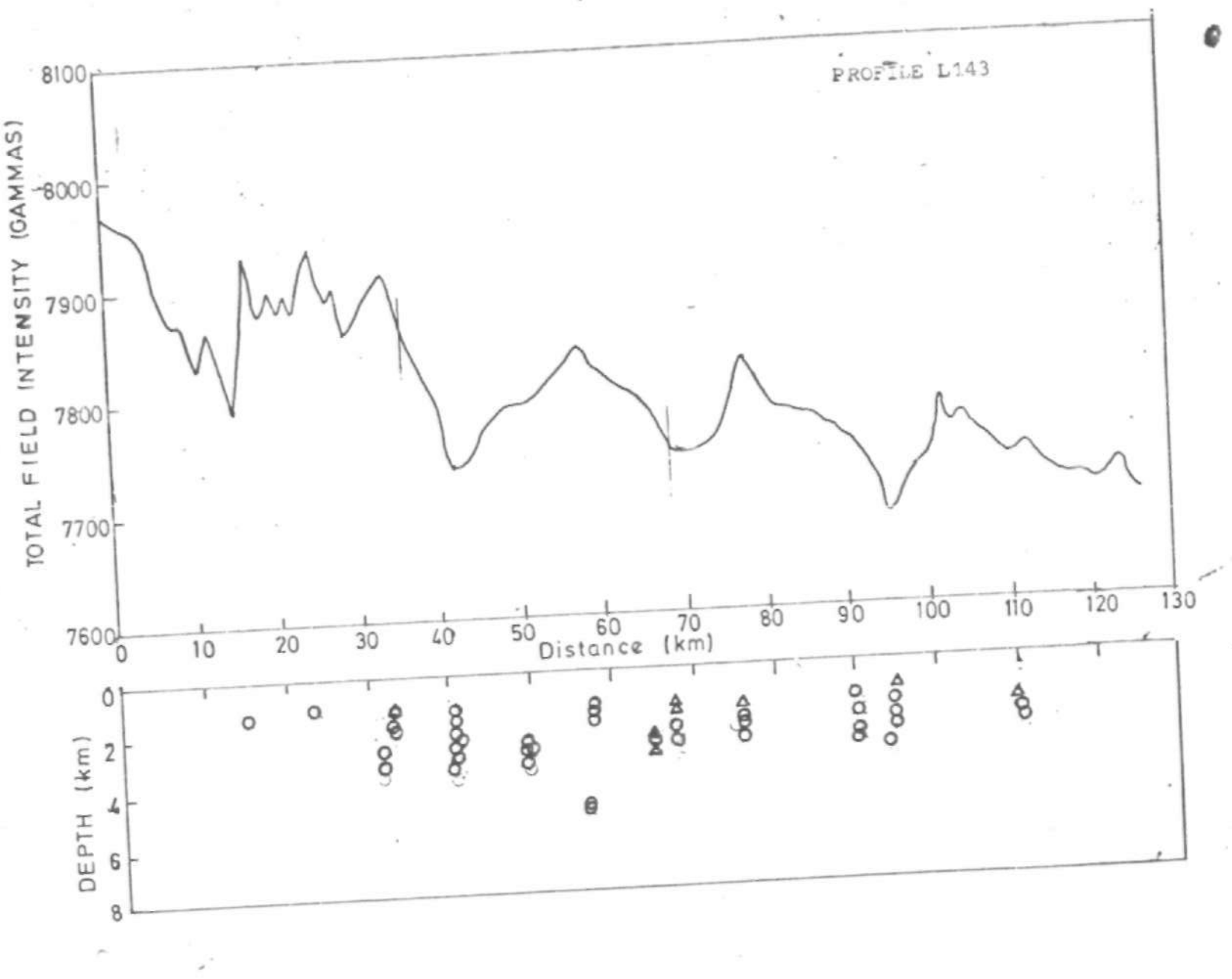

PROFILE L132
TOTAL FIELD INTENSITY (GAMMAS)
8000
7950
7900
7850
7800
7750
7700
7650
7600
0
10
20
30
40
50
60
70
80
90
100
Distance (km)
DEPTH (km)
0
2
4
6
8

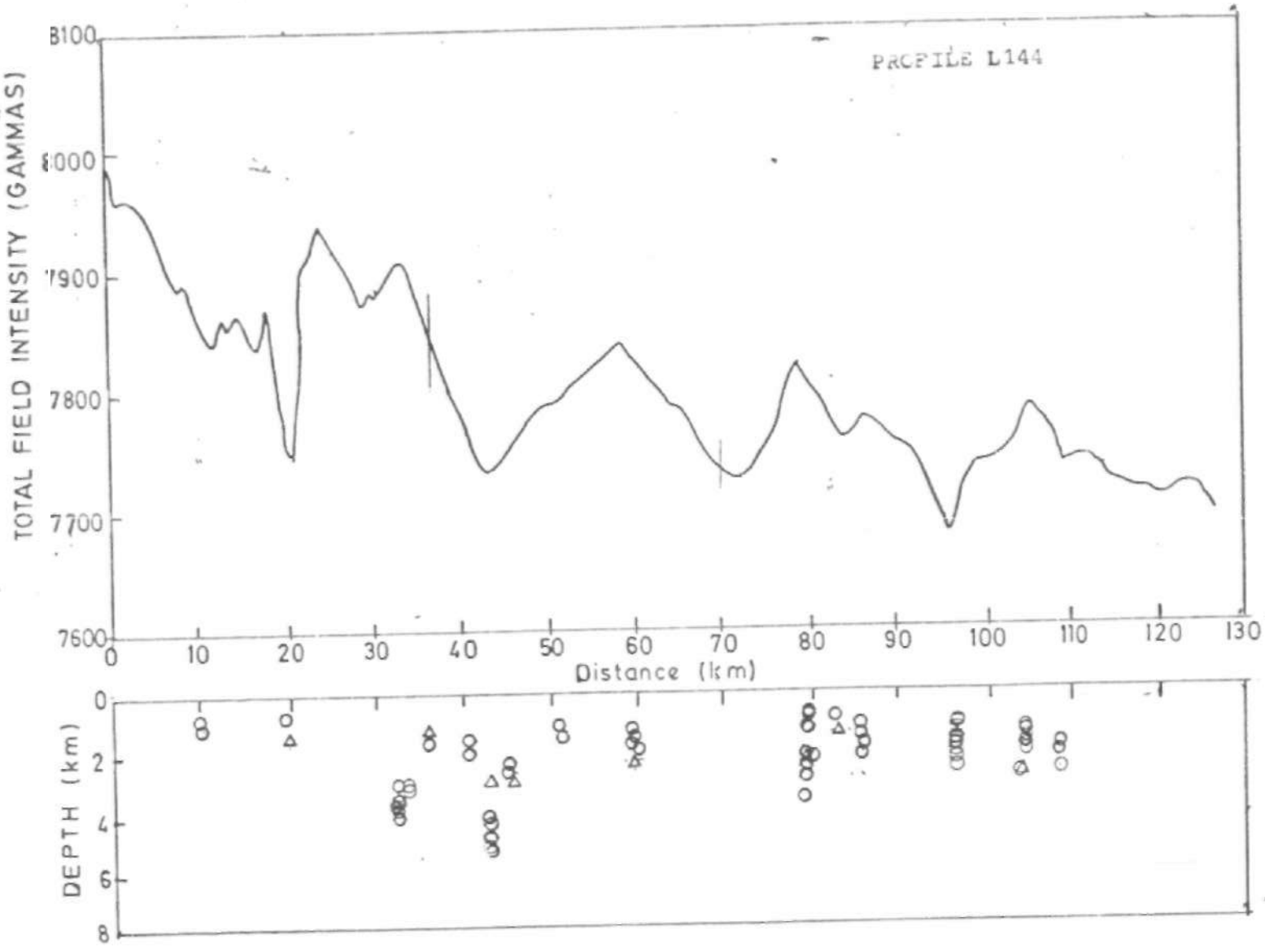

PROFILE L133
TOTAL FIELD INTESITY (GAMMAS)
8000
7950
7900
7850
7800
7750
7700
7650
7600
0
10
20
30
40
50
60
70
80
90
100
Distance (km)
DEPTH (km)
0
2
4
6
8

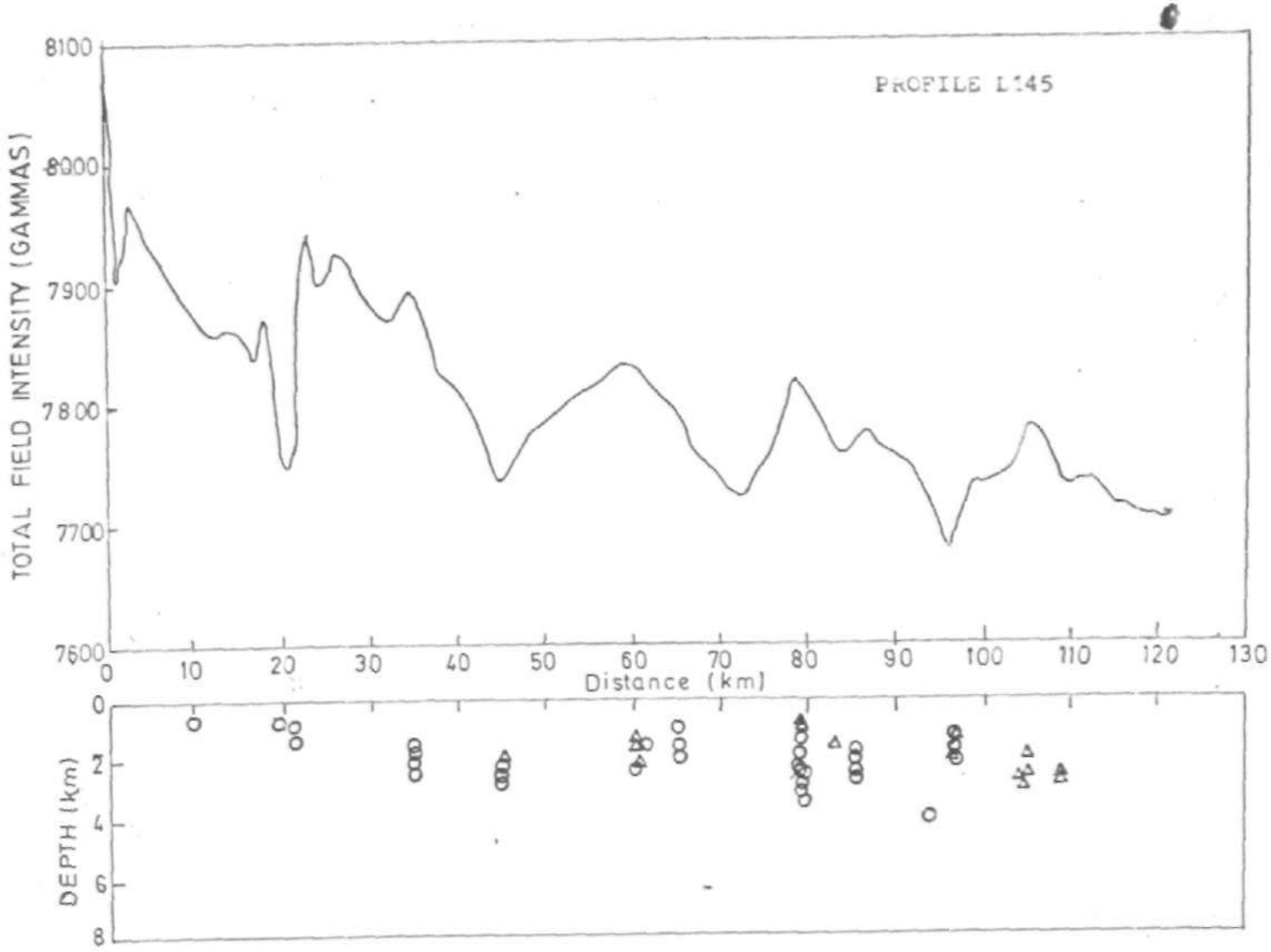

PROFILE L134
TOTAL FIELD INTENSITY (GAMMAS)
8000
7950
7900
7850
7800
7750
7700
7650
7600
0
10
20
30
40
50
60
70
80
90
100
110
120
Distance (km)
DEPTH (km)
0
2
4
6
8

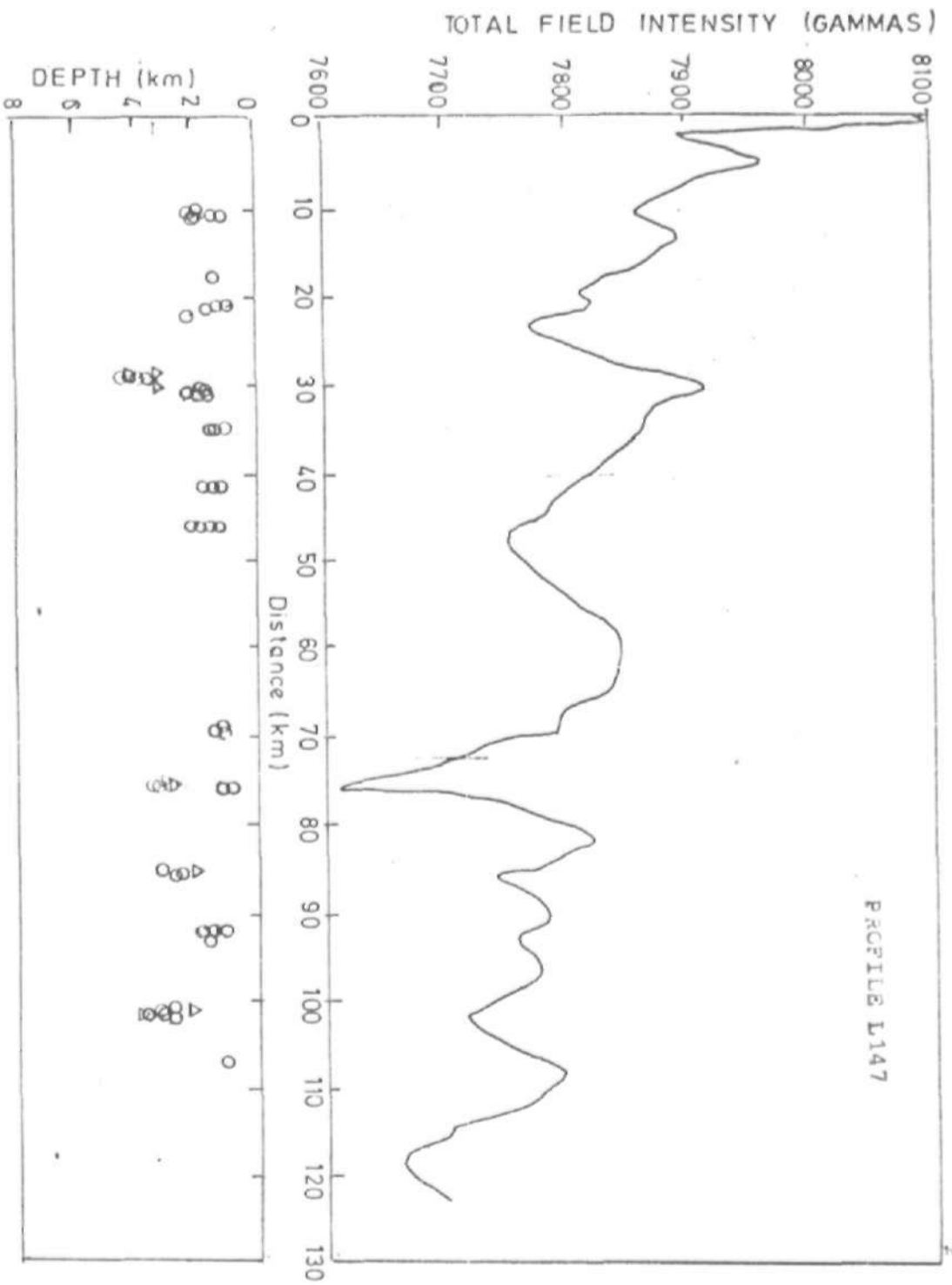

PROFILE L141
TOTAL FIELD INTENSITY (GAMMAS)
8100
8000
7900
7800
7700
7600
0
10
20
30
40
50
60
70
80
90
100
110
120
130
Distance (km)
DEPTH (km)
0
2
4
6
8

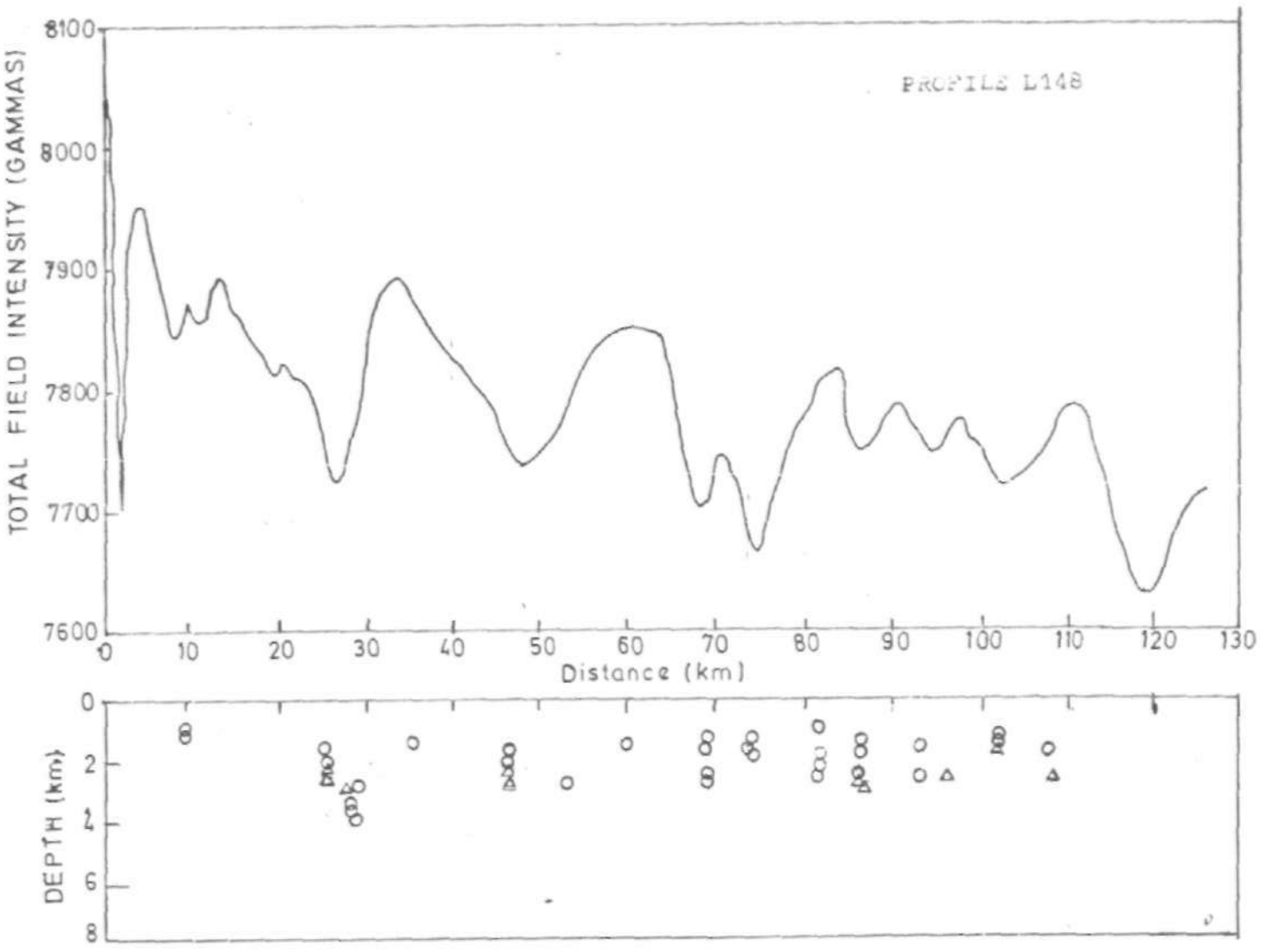

PROFILE L142
TOTAL FIELD INTENSITY (GAMMAS)
8100
8000
7900
7800
7700
7600
0
10
20
30
40
50
60
70
80
90
100
110
120
130
Distance (km)
DEPTH (km)
0
2
4
6
8

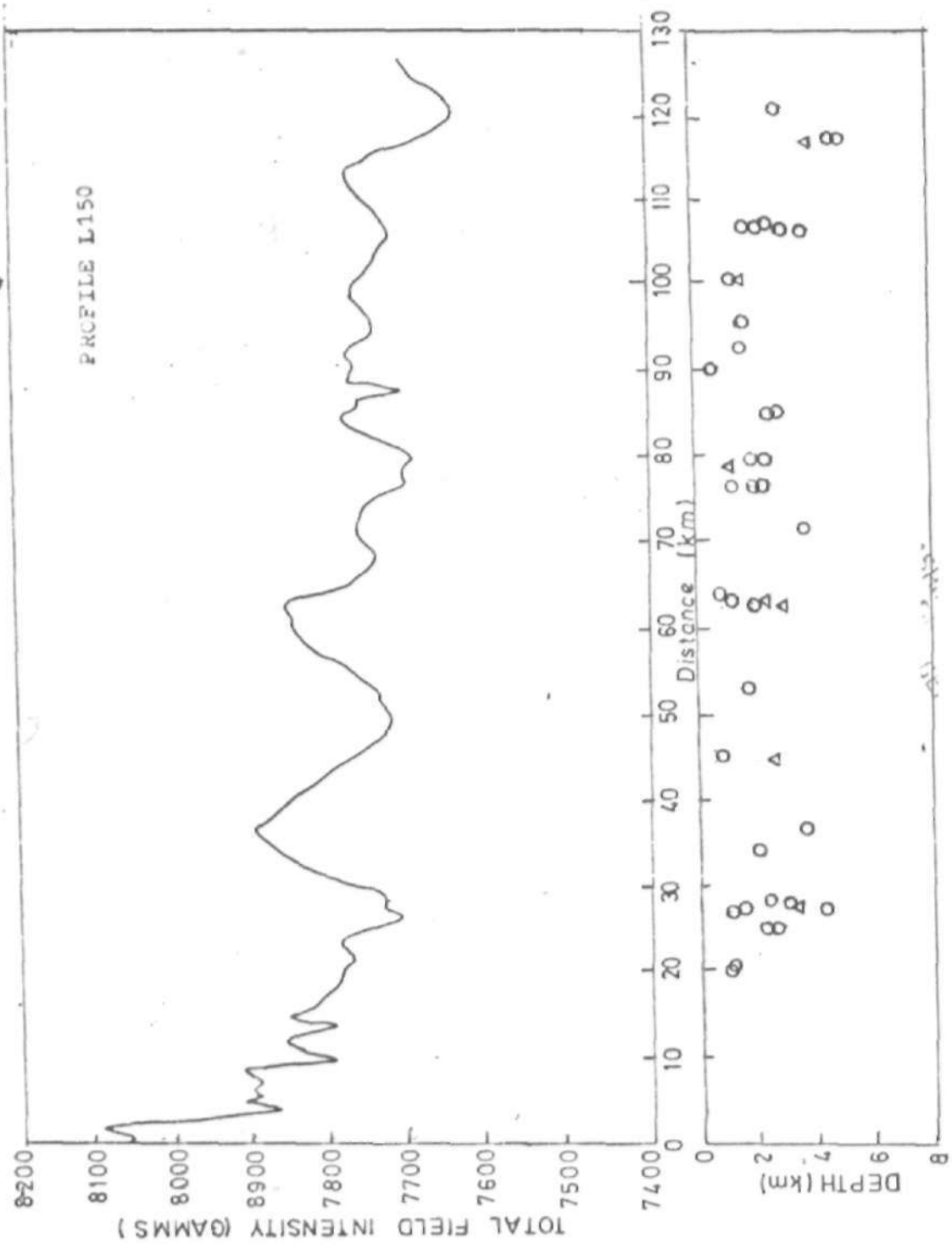

PROFILE L143
TOTAL FIELD INTENSITY (GAMMAS)
8100
8000
7900
7800
7700
7600
0
10
20
30
40
50
60
70
80
90
100
110
120
130
Distance (km)
DEPTH (km)
0
2
4
6
8


PROFILE L144
TOTAL FIELD INTENSITY (GAMMAS)
8100
8000
7900
7800
7700
7600
0
10
20
30
40
50
60
70
80
90
100
110
120
130
Distance (km)
DEPTH (km)
0
2
4
6
8


PROFILE L145
TOTAL FIELD INTENSITY (GAMMAS)
8100
8000
7900
7800
7700
7600
0
10
20
30
40
50
60
70
80
90
100
110
120
130
Distance (km)
DEPTH (km)
0
2
4
6
8


TOTAL FIELD INTENSITY (GAMMAS)
7600
7700
7800
7900
8000
8100
0
10
20
30
40
50
60
70
80
90
100
110
120
130
PROFILE L147
DEPTH (km)
8
6
4
2
0
Distance (km)


PROFILE L148
TOTAL FIELD INTENSITY (GAMMAS)
8100
8000
7900
7800
7700
7600
0
10
20
30
40
50
60
70
80
90
100
110
120
130
Distance (km)
DEPTH (km)
0
2
4
6
8


PROFILE L150
TOTAL FIELD INTENSITY (GAMMAS)
8200
8100
8000
7900
7800
7700
7600
7500
7400
Distance (km)
0
10
20
30
40
50
60
70
80
90
100
110
120
130
DEPTH (km)
0
2
4
6
8